A coupling of the origin of asteroid belt, planetary ring, and comet

Yongfeng Yang

Bureau of Water Resources of Shandong Province, Jinan, Shandong Province, China, Mailing address: Shandong Water Resources Department, No. 127 Lishan Road, Jinan, Shandong Province, China, 250014

Tel. and fax: +86-531-8697-4362

E-mail: roufengyang@gmail.com

Abstract

It has been confirmed that there are an asteroid belt, four giant planetary ring systems, and countless comets in the solar system. Various scenarios had been previously presented to account for their origin, but none of them is competent. Asteroid belt located between the orbits of Mars and Jupiter is flat, circular, and parallel to the ecliptic, similarly, planetary ring located between the orbits of satellites is also flat, circular, and approximately parallel to its planetary equatorial plane. This similarity implies that asteroid belt and planetary ring are likely to derive from a common physical process. Here we propose 5 significant collisional events of the two bodies of binary planetary (satellite) system in the history of the solar system. In each event, the two bodies are shattered into fragments toward all around. Due to the confinement of hierarchical two-body gravitation (non-Newton's gravitation), the barycenter of initial binary system was survived in the collision, and all fragments ejected were still organized in a series of hierarchical two-body systems. As inferred from Galileo's experiment of projectile, the fragments automatically run some parabolic trajectories in space. But at the same time, the survived barycenter continued to drag these fragments by means of the barycenters of a series of subordinate two-body systems to orbit, by which these fragments were gradually confined to fall on a circular belt (ring). The interaction of radial immigration and vertical falling makes the belt (ring) of fragments flat. Some of the fragments may be further shattered into very small fragments (particles with a size of meter

or micron, for instance) to form independent belts (rings). The collision between the two bodies of a binary planetary system gives birth to the asteroid belt, while the collision between the two bodies of a binary satellite system gives birth to the giant planetary ring system. Some further fragments (relative to the collisional origins) bombard the objects they encounter in travel and leave craters on the surfaces. Due to the motions of the survived barycenter around the Sun (giant planet) and giant planet around the Sun, the further fragments are brought to run through the solar system back and forth, this results in the advent of comets when close enough to the Sun, and appearance of meteors when close enough to the Earth, some of the fragments occasionally landed on the surfaces of planets and satellites and become meteorites.

1 Background

Long-term ground and spacecraft-based observations confirm that there are an asteroid belt, four giant planetary ring systems, and countless comets in the solar system. A great number of scenarios had been proposed in the past to account for their origin. The origin theories of planetary ring are plentiful. Especially for the Saturn's ring, they include tidal disruption of a small moon (Roche et al. 1847), unaccreted remnants from the satellite-formation era (Pollack et al. 1976), collisional disruption of a small moon (Charnoz et al. 2009), and tidal disruption of a comet (Dones 1991). Canup (2010) concluded the disabilities of these theories and developed a model of planetary tidal force striping ice material from a Titan-sized satellite. The previous origin theory of asteroid belt believes that asteroids are fragments of a destroyed planet (Herschel 1807), the currently accepted scenario believes asteroids to be the rocks that in primordial solar nebula never accumulate into a genuine planet (Petit et al.2001). The origin theory of comet mainly includes Oort cloud hypothesis that proposes a cloud of comets at the outer reaches of the solar system (Oort 1950) and Kuiper belt hypothesis that proposes a disc shaped region of space outside the orbit of Neptune to act as a source for short-period comets (Kuiper 1951). However, a large number of observations of the planetary ring and asteroid belt are strongly questioning these established scenarios. If the Saturn's rings are from a previous pure ice ring as Canup proposed (2010), it is necessary for them to hold identical material, but observation shows that the Saturn's rings have various spectral characteristics and these features are interlacing in spatial distribution. This kind of strange distribution is hard to be created by any natural contamination from

interstellar matter. To support the production of icy moons, Canup further employed another work by Charnoz et al (2010) that ring material spreading beyond the Roche limit may accrete to form icy moons. But the Roche limit itself is doubtful because a lot of satellites whose distances from their father planets (Jupiter, Uranus, and Neptune, for example) are interior to the Roche limit are still existed (Burns et al. 2001). The Saturn's rings are very broad and divided by many divisions that look like natural boundaries, the particles in each ring appear to orderly orbit and never ride over these boundaries. This requires a longitudinal confining mechanism to be responsible for.

We also see a big difficulty in understanding the Uranus's rings and Neptune's ring arcs. The Uranus possess more than 13 narrow rings, this needs some mechanism to hold these bodies together. Goldreich and Tremaine (1979) proposed a series of small satellites exerting gravitational torques to confine the Uranus' rings. To be effective, the masses of the satellites need to exceed the mass of the ring by at least a factor of two to three (Porco et al. 1987). But only the ε ring is latterly observed to have two small companions - Cordelia and Ophelia, no satellite larger than 10 km in diameter is known in the vicinity of other rings (Smith et al. 1986). The Neptune's ring arcs currently keep unresolved (Miner et al. 2007), even if a large number of models (Smith et al.1989; Salo and Hnninen 1998; Dumas et al. 1999; Sicardy et al. 1999; Namouni and Porco 2002; Renner and Sicardy 2003 and 2004) in the past 20 years had been attempted.

Herschel's idea of the formation of asteroid belt (1807) was rejected due to its disability in explaining the supply of shattering energy and the diversity of asteroids' composition. The widely accepted thought proposed by Petit et al (2001) is that the asteroids are the planetesimals that were left from primordial solar nebula. This plausible thought, however, is strongly against an observational fact. A large number of asteroids in the belt belong to some families (or groups), in which these asteroids share not only similar chemical composition but also similar orbital elements such as semi-major axis, eccentricity, and orbital inclination. If the asteroids are the planetesimals of primordial solar nebula, any random movement between the planetesimals will not allow those who hold similar chemical composition to cluster into a physical association. So far, around one-third of the asteroids in the asteroid belt have been confirmed to be the members of an asteroid family. Given the limitation of observation, we still have chance to classify more asteroids into some families. Most importantly, the nebula hypothesis itself is being seriously surrounded by a series of problems such as the loss of angular momentum, the disappearance of

the disk, the formation of planetesimals, the formation of giant planets and their migration, and so on (Woolfson 1993; Taishi et al. 1994; Andrew et al. 2002; Klahr and Bodenheimer 2003; Inaha et al. 2003; Wurchterl 2004), the planetesimal therefore is nothing but a hypothesis of hypothesis.

The comet's two origin theories are also questionable. Jan Oort (1950) statistically found that there is a strong tendency for aphelia of long period comet orbits to lie at a distance of about 50,000 AU and then concluded that comets reside in a vast cloud at the outer reaches of the solar system. It is very important to note that this so-called aphelia of comet orbit is derived from Keplerian expectation other than observation, nobody in person sees that the aphelia of a comet's orbit is indeed located at such a distant place. In practice, when we observe a comet, the Earth is rotating around its axis, at the same time the Earth-Moon system is also rotating, and the barycenter of the Earth-Moon system is also revolving around the Sun, what we see is a compositive motion for the comet. In other words, it is rather difficult to determine the comet's proper motion. In addition to this, the solar system itself is flat, it appears to be no reason for people to believe there will have a spherical cloud of comets at the outer reaches of the solar system. On the other hand, the orbital features of short period comets do not approve an origination from Oort cloud, and the mechanism by which the comets are supplied from Kuiper belt to planet-crossing orbits is still unclear (Duncan et al. 1988). In the last 20 years, though a lot of Trans-Neptunian objects had been found from the proposed Kuiper belt, there is no evidence to show that these Trans-Neptunian objects are really linked to comets. The recent discovery of main belt comets (Hsieh et al. 2006) indicates that the origin of comet is likely to be different from the expectation of conventional knowledge.

In conclusion, the established origin theories of asteroid belt, planetary ring, and comet are so questionable that we need to run a full consideration. Both asteroid belt and planetary ring are flat, circular, and parallel to respectively the ecliptic and planetary equatorial plane; they are embedded respectively in planetary orbits and in satellites' orbits; In addition to this, asteroids consist primarily of carbonaceous, silicate, and metallic materials, which is similar to the composition of Earth and Mars. Relatively, planetary ring consists primarily of ice and dust, which is similar to the composition of icy satellites. On large scale, the Sun has a number of planets, each giant planet (Jupiter, Saturn, Uranus, and Neptune) also has a number of satellites. This similarity suggests that the formation of asteroid belt and planetary ring should share a common physics. On the other

hand, the Saturnian F ring and the Uranian ε ring are both narrow, and are generally shepherded by a pair of moons (Esposito 2002), the outer rings of Uranus are similar to the outer G and E rings of Saturn (Pater et al. 2006), narrow ringlets in the Saturnian rings also resemble the narrow rings of Uranus, the Neptunian ring system is quite similar to that of Uranus (Esposito 2002; Burns et al. 2001). This similarity suggests that four giant planets' ring systems are likely to be ruled by a common physics. Other observations of crater, star, extraplanet, and satellite offer us significant suggestion. The craters on the surfaces of planets and satellites indicate that it had taken place some great bombardment events in the history of the solar system. The analysis of impact crater record further confirms an inner solar system impact cataclysm occurred 3.9 Gy ago (Strom et al. 2005), while the heavily crater surfaces on Ganymede and Gallisto confirms other impact cataclysms occurred in the outer solar system (Strom et al. 1981). These impact cataclysms naturally require different projectile origin at different time to be responsible for. A number of observations have confirmed a fact that the orbit of celestial object is generally decreasing. The two stars in binary star system RX J0806.3+1527 are found to be steadily decreasing orbital period at a rate of 1.2 milliseconds per year. The orbital period of binary star Cen X-3 and SMC X-1 is decreasing at a rate of respectively Porb/Porb = 1.8 x 10^{-6} yr^{-1} and 3.36x 10^{-6} yr^{-1}(Kelley et al. 1983; Levine et al. 1993). PSR B1913+16 have a rate of decreasing orbital period of 76.5 microseconds per year, and the rate of decrease of semimajor axis is 3.5 meters per year (Weisberg and Taylor 2004). Many hot giant planets are detected to be revolving around stars with very short-period orbits. The members of "51 Peg" planets, 51 Peg itself, Tau Bootis, 55 Cancri, and Upsilon Andromedae, have orbital periods of just 4.2, 3.3, 14.7, and 4.6 days, respectively, and their orbits are very small, with radii less than 0.11 AU. A steamy planet is recently found to be orbiting a faint star with a distance of just 1.3 million miles (Terquem and Papaloizou 2007). This short-period orbit suggests that these extrasolar planets could have been giant icy planets formed far enough from their stars that ices could condense, and then have migrated towards their stars (Brunini and Cionco 2005; Raymond et al. 2008; Charbonneau et al. 2009). The moon of Mars, Phobos has a decreasing orbit at a rate of 1.8 cm/yr (Clark 2010). So far, there is very little evidence to show that the orbit of celestial object is increasing, especially for planet and satellite, and because the effect of gravitation is to drag objects to approach each other, we thus have reason to infer that the decrease in celestial object's orbit is necessary, even if it is difficult to be detected

during a short period of time. A decreasing orbit destines an increase in orbital velocity and a catastrophic collision between two bodies. In addition to these, the well-regulated movement of asteroid family (group) (Hirayama 1918), the integrity of the Saturn's narrow F ring (Murray et al. 2008), and the twisted arc in the Neptune's Adams ring (Hammel 2006) appear to indicate that they do not obey the constraint of Newton's gravity. Yang (2011) recently introduced a model to show that all objects in the universe are initially built up from small units (ordinary particles) through a pattern of one-capture-one and therefore organized in a series of hierarchical two-body systems to orbit, and that the two bodies of a two-body system due to orbital decrease will eventually take place a collision. A natural result from the collision of two bodies is to shatter them into small fragments, these fragments may further bombard the objects they encounter in travel, but under the effect of hierarchical two-body gravitation they may be confined to fall on a circular belt. Some of them, if hold volatile material and close to the Sun, may become comets. In this present paper, we totally formulate 5 physical collisional scenarios of the two bodies of binary planetary (satellite) system to clear up all suspicions above at the same time and further account for some observations.

2 Modelling

According to the work by Yang (2011) that every celestial object is initially built up from small units by means of a pattern of hierarchical two-body capture. This means that if a celestial object is reversely shattered into fragments, these fragments are still gravitationally constrained in a series of hierarchical two-body systems and the barycenter of initial celestial object may be survived. Based on this physics, a conceptual model is developed to formulate the formation of a belt (ring system) (Fig.1): A two-body system is orbiting a center body; With the passage of time, the two bodies of the two-body system due to orbital decrease occur a smashing collision and are shattered into fragments. But due to the constraint of hierarchical two-body gravitation, the barycenter of the initial two-body system is survived in the collision, and all fragments are still organized in a series of hierarchical two-body systems; The barycenter continues to drag these fragments by means of the barycenters of a series of subordinate hierarchical two-body systems to orbit, by which all fragments are gradually confined into a circular belt (ring). As shown in Figure 1(D), the barycenter of initial two-body system (point *O*) is dragging two components (point *a* and 1) to orbit, at the same time point *a* is also dragging two components (point *b* and *d*) to orbit, point

b is also dragging two components (point *c* and one fragment) to orbit, etc. Because of this successive hierarchical drag from point *O* to related points, all fragments can always obtain some displacements to radially approach the orbit of point *O*. With the passage of time, they will have to be confined to fall on a circular belt (ring). It is necessary to note that, because Galileo's experiment of projectile shows the projectile runs a parabolic trajectory in space, and because all fragments ejected from this collisional event are constrained in a series of hierarchical two-body systems, this means every fragment will run a parabolic trajectory round a barycenter. As shown in Figure 1(D), the fragment (M) will run a parabolic trajectory around the barycenter (point *e*). Because of orbital decrease, the survived barycenter of the initial two-body system is increasingly approaching the center body, this leads the fragments by means of the barycenters of a series of subordinate hierarchical two-body systems to move toward the center body, the belt (ring) slowly becomes flat.

We here formulate one collision of binary planetary system and four collisions of binary satellite system in the history of the solar system. For the collision of binary planetary system, the center body is replaced with the Sun, the composition and mass of the binary planetary system is similar to that of the Earth-Moon system, and it is located between the orbits of the Mars and Jupiter. The collision occurred at the time of Late Heavy Bombardment. After the collision, all fragments are ejected towards all around. Due to the successive hierarchical drag, all fragments are confined to gradually fall on a circular belt (ring). Some distant fragments (with respect to the collisional source), because of the motion of the survived barycenter around the Sun, are brought to run across the solar system back and forth. Water is froze along with the fragments, atmosphere is either escaped or sealed in the bodies of the fragments. This collision mainly gives birth to the asteroid belt. For the four collisions of binary satellite system, the center body is replaced with Jupiter, Saturn, Uranus, and Neptune, respectively, the composition and mass of each binary satellite system is similar to that of icy satellite of each giant planet, and it is located between the orbits of the planet and its major satellite. The four collisions of binary satellite system occurred generally later than the time of Late Heavy Bombardment. After the collision, all fragments are ejected towards all around. Due to the successive hierarchical drag, all fragments are confined to gradually fall on a circular belt (ring). The falling fragments due to dynamical collision are further shattered into very small fragments (particles with a size of meter or micron, for instance) that are

still constrained in a series of subordinate hierarchical two-body systems, and thereby form many individual belts (rings). Some distant fragments (with respect to the collisional source), because of the motion of the survived barycenter around the planet and the planet around the Sun, are brought to run across the solar system back and forth. These four collisions mainly give birth to the giant planet's ring systems.

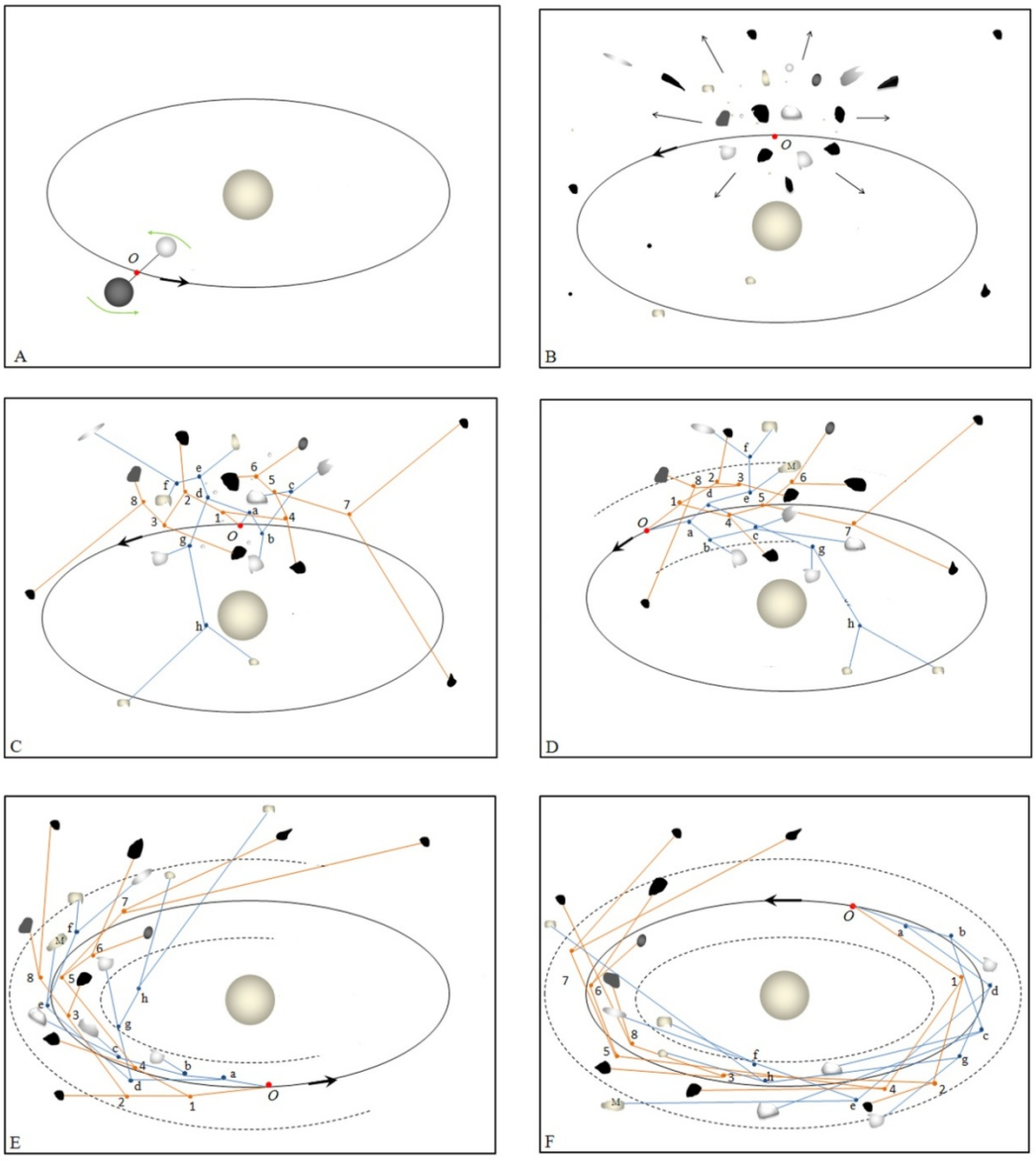

Figure 1: Simulation of the formation of a belt (ring system) based on hierarchical two-body gravitation. From A, B, C, D, E to F, it demonstrates the formation of a belt (ring system). Point *O* (marked with red dot) denotes the barycenter of initial two-body system. Blue (orange) dots (marked with letter *a*, *b*, *c*, etc., and number 1, 2, 3, etc.) represent the barycenters of related two-body systems in the associations. Blue (orange) line represents gravitation. Large black arrow represents the motion

of the integral association. Dashed circle denotes the boundary of the belt (ring system).

3 Match with observation

3.1 Asteroid belt

Long-term observation shows that a large number of irregularly shaped bodies are occupying a wider region that is located approximately between the orbits of the Mars and Jupiter. In general, the majority of these bodies are clustered in a belt of 2.15 to 3.3 AU from the Sun. Over 200 known asteroids in the belt are larger than 100 km (Tedesco and Desert 2002). Data from Minor Planets Center shows that a population of 700,000 ~ 1.7 million asteroids are with a diameter of 1 km or more. The belt is proved to be composed primarily of three categories of asteroids: C-type or carbonaceous asteroids, S-type or silicate asteroids, and M-type or metallic asteroids, and that approximately one-third of the asteroids in the belt belong to some certain families (or groups), in which they share similar chemical composition and orbital elements, such as semimajor axis, eccentricity, and orbital inclination. Three bands of dust within the main belt have also been found to share similar orbital inclinations as the Eos, Koronis, and Themis asteroid families (Love et al. 1992). Data from Minor planets Center shows that most asteroids within the asteroid belt have large orbital eccentricities and various orbital inclinations.

Reference to Figure 1, it can be inferred that the fragments rejected from the collision of the two bodies of the binary planetary system must be irregularly shaped, and that under the hierarchical two-body confinement, these fragments will be gradually dragged to fall on a circular belt around the Sun. A natural result from the collision is the majority of the fragments must be small in size. The chemical composition of the binary planetary system is similar to that of the Earth-Moon system, this means that the fragments ejected from the binary planetary system are composed of mainly C-type or carbonaceous, S-type or silicate, and M-type or metallic materials. It can also be inferred that some fragments may be further shattered into small fragments that are still constrained in a series of hierarchical two-body systems, this forms an association of small fragments that may be called a family or group. As every fragment is dragged by a barycenter to orbit, and the barycenter is further dragged by the barycenter of a superior two-body system to orbit, this determines that the fragments in a common association must share identical orbital elements such as eccentricity, period, and inclination. Also because the fragments in a common

association are derived from the disruption of a common parent body, this determines them to be with identical composition. Figure 2 shows an artistic configuration of the asteroid belt, in which all fragments (asteroids) are being organized in a series of hierarchical two-body systems to orbit.

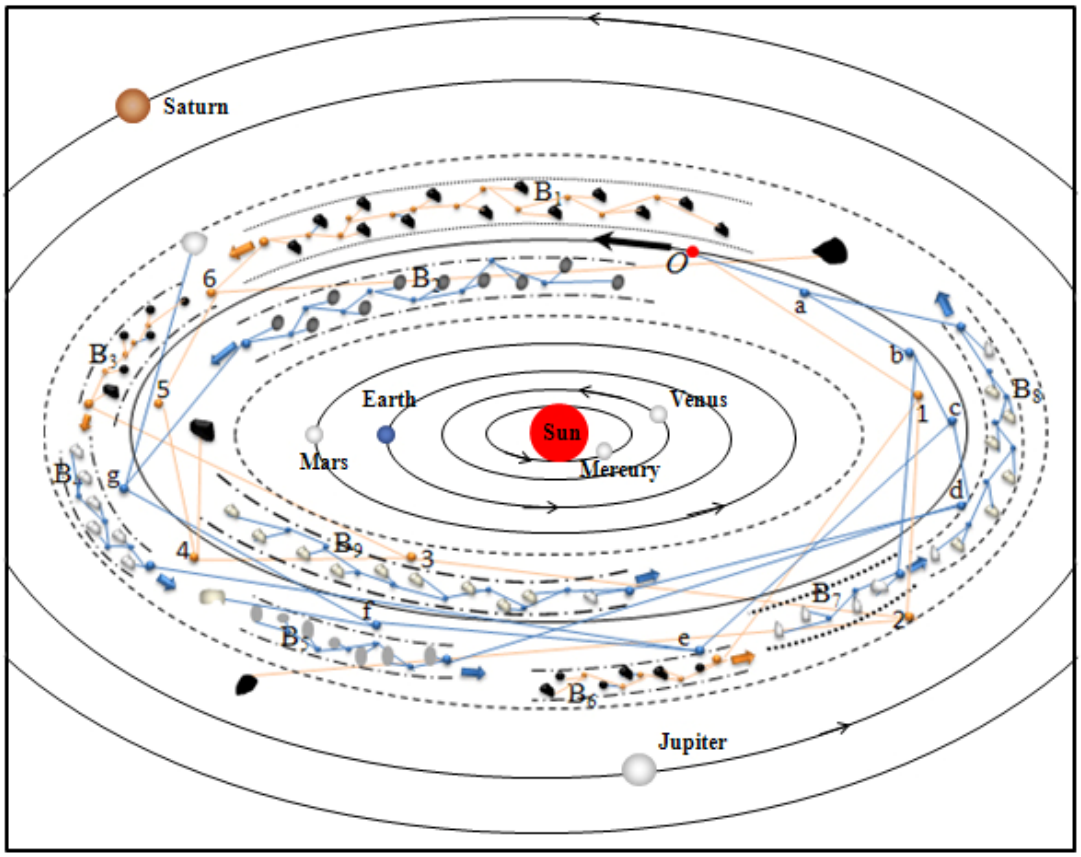

Figure 2: A hierarchical two-body association of fragments (asteroid) for the asteroid belt. The span of two dashed circles is the region occupied by the asteroid belt. Different color in the fragment denotes different composition. Point *O* (marked with red dot) denotes the barycenter of asteroid belt. B_1, B_2, B_3 etc. denote asteroid families that consist of a series of subordinate hierarchical two-body systems of smaller fragments (asteroids). Blue (orange) dots (marked with letter *a*, *b*, *c*, etc., and number 1, 2, 3, etc.) represent the barycenters of related superior two-body systems that control these families through gravitation. Blue (orange) line represents gravitation in. Large black arrow represents the mean motion of the asteroid belt, while short blue (orange) arrow represents mean motion of each family.

The formation of asteroid belt here is numerically determined. However, before the beginning of this work, we must know a fact that at the moment when the collision of the two bodies of the binary planetary (satellite) system occurs, all fragments and barycenters (including barycenter *O*) must instantaneously hold one inertial motion, while the collision subsequently

gives each of them another motion. This means, the final motion of each fragment (barycenter) is a consequence of the interaction between the two motions and gravitation. This may be approximately thought that each fragment is being dragged to run a parabolic trajectory around the gravitation origin (Fig.3). Because of this property of motion, the fragments (asteroids) within the belt are determined to be with the orbits of high eccentricities and various inclinations.

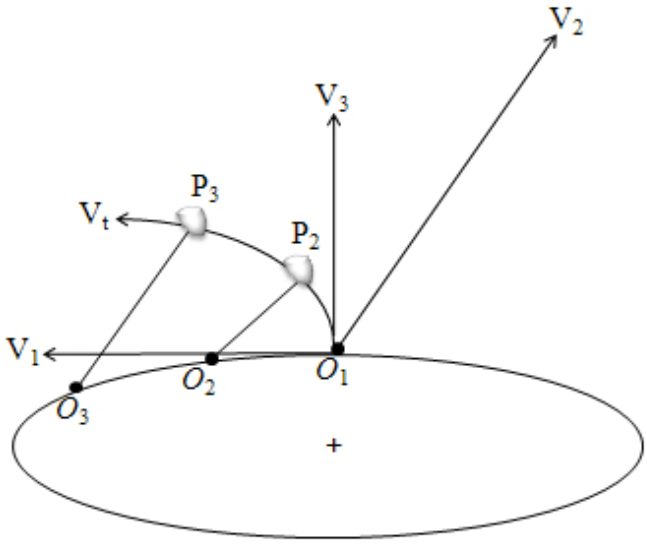

Figure 3: Fragment's motion under the interaction of inertial motion and gravitation. A fragment is ejected from a gravitation origin O_1, at the moment the fragment's inertial motion is V_1 that is tangential to the position of O_1, the motion obtained from the collisional ejection is V_2, the compositive motion between the two is V_3, but because of the effect of gravitation that is from the origin O_1 and the origin is in motion along a path O_1-O_2-O_3, the fragment is therefore dragged to run a parabolic trajectory of O_1-P_2-P_3.

And then, we assumed that the interaction of inertial motion and ejection motion has been determined well and that all fragments ejected are organized into a series of hierarchical two-body systems. As the barycenter (point *O*) is survived in the collision and continues to orbit, it drags all fragments to move by means of the barycenters of a series of subordinate hierarchical two-body systems (Fig. 4(A)). A natural result is that all fragments are eventually confined to fall on a circular belt around the center body. To specify this confinement, we define a three-dimensional Cartesian coordinate system, in which the barycenter (point *O*) is the origin, *xoy* plane is parallel to the orbital plane of the barycenter, and *zoy* plane is vertical to the orbital plane. We assumed

that two branches of fragments are flatly distributed at *xoy* plane that is parallel to the ecliptic, while another two branches of fragments are flatly distributed at *zoy* plane that is vertical to the ecliptic (Fig. 4(B)). It has been proposed that all objects are organized into a series of hierarchical two-body systems to orbit, and the gravitation between them is expressed through the barycenters of these two-body systems (Yang 2011). This means that the Sun and planets are indirectly attracting these fragments through the barycenters of these two-body systems. But because the Sun relative to planet has a very massive mass, the gravitational effect of all planets on each fragment may be neglected, the Sun may be treated as the only gravitation origin.

According to (Fig. 4(B)), the motion of each fragment (barycenter) may be expressed as

$$V_t = \sqrt{{V_0}^2 + (at)^2 - 2 \times V_0 \times at \times \cos\alpha} \quad (1)$$

$$\mathrm{S}_t = \frac{1}{2} \times a \times t^2 \quad (2)$$

$$\mathrm{X(Z)}_t = \mathrm{S}_t \times \cos\beta \quad (3)$$

Where a represents acceleration encountered by a fragment (barycenter), V_0 the initial velocity of the fragment at the moment when the collision occurs (which is virtually a consequence of the interaction of inertial motion and ejection motion), V_t the orbital velocity of the fragment (barycenter) after a time of *t*, S_t the displacement of the fragment (barycenter) in the direction of acceleration, $\mathrm{X(Z)}_t$ the displacement of the fragment (barycenter) in the direction of *x* (*z*) axis, α the angle between the initial velocity and acceleration, β the angle between *x* axis and acceleration.

In this case, for example, at any moment fragment M_9 encounters an acceleration that is from the gravitation of all other fragments and the Sun, the Sun's gravitation runs a path of Sun-*O*-a-d-e-f-M_9, therefore the gravitational distance between the Sun and M_9 is $r_{\text{Sun-M9}} = L_{\text{Sun-}O} + L_{O\text{-a}} + L_{\text{a-d}} + L_{\text{d-e}} + L_{\text{e-f}} + L_{\text{f-M9}}$, while fragment M18's gravitation runs a path of M_{18}-7-5-4-1-*O*-a-d-e-f-M_9, which corresponds to a gravitational distance of $r_{\text{M18-M9}} = L_{\text{M18-7}} + L_{7\text{-}5} + L_{5\text{-}4} + L_{4\text{-}1} + L_{1\text{-}O} + L_{O\text{-a}} + L_{\text{a-d}} + L_{\text{d-e}} + L_{\text{e-f}} + L_{\text{f-M9}}$. The fragment's initial velocity is V_o, the acceleration is in the direction of line M_9-f, the interaction of initial motion and acceleration thus makes M_9 move momentarily in the direction of line M_9-D, even if the acceleration can contribute some work to make M_9 move towards the indirection of *y* axis. This situation is the same for all other fragments.

The acceleration is determined by an experienced method, because if we simply treat g = a (where g is gravitational acceleration), the Sun will swallow the Earth quickly, for instance, this is obviously not the fact. But we can feel, the acceleration is essentially rooted from a cause of gravitation, therefore there must be a relation between them. In another work (unpublished), I employ a geological record of coral fossil to estimate planet's orbital decreasing rate, which indirectly reflects the relation of acceleration and gravitation. The orbital decreasing rate for the Earth is $\Delta R_{earth} = 12.15 \times 10^{-5} \times t + \frac{1}{2} \times 8.3681 \times 10^{-16} \times t^2$ km (where the unit of t is in days). Assumed that the orbital decreasing rate is exponentially relative to gravitational distance and mass that is from the same gravitation origin, the orbital decreasing rate for the barycenter (point O) in this paper may be expressed as $\Delta R_O = (\frac{R_{earth}}{R_O})^2 \times \Delta R_{earth}$ (where Ro for the asteroid belt is 2.67 AU). As the collision of the binary planetary system occurred 3.9 billion years ago, this means, at the moment the orbital radius of the binary planetary system (relative to the Sun) is R = 2.67 (present) + $0.14 \times \Delta R_{earth}$ (past) = 4.13 AU, which is equal to $L_{Sun\text{-}O}$. We further define $\Delta R_O = \bar{a}t$ to obtain an average acceleration for the barycenter (point O). As all fragments (barycenters) are constrained by the same gravitation origin-the Sun, the acceleration for each fragment (barycenter) may be further written as $a = \bar{a} \times (\frac{L_{Sun-O}}{L_{Sun-fragment}})^2$. It is assumed that initial velocity $V_0 = \sqrt{\frac{GM_{Sun}}{L}}$ (where G is gravitational constant, M_{Sun} is the Sun's mass, L the distance of fragment and the Sun). The initial positions of fragments (barycenters) and their mass are assigned in Table 1, the unit of the coordinate axis is AU and 1 AU =149 598 000 Km, and given the gravitation between any two fragments is slight if their distance is large enough, the Sun's gravitation is the only one that attracts each fragment. The motions of all fragments out to time are thus determined (Fig.5).

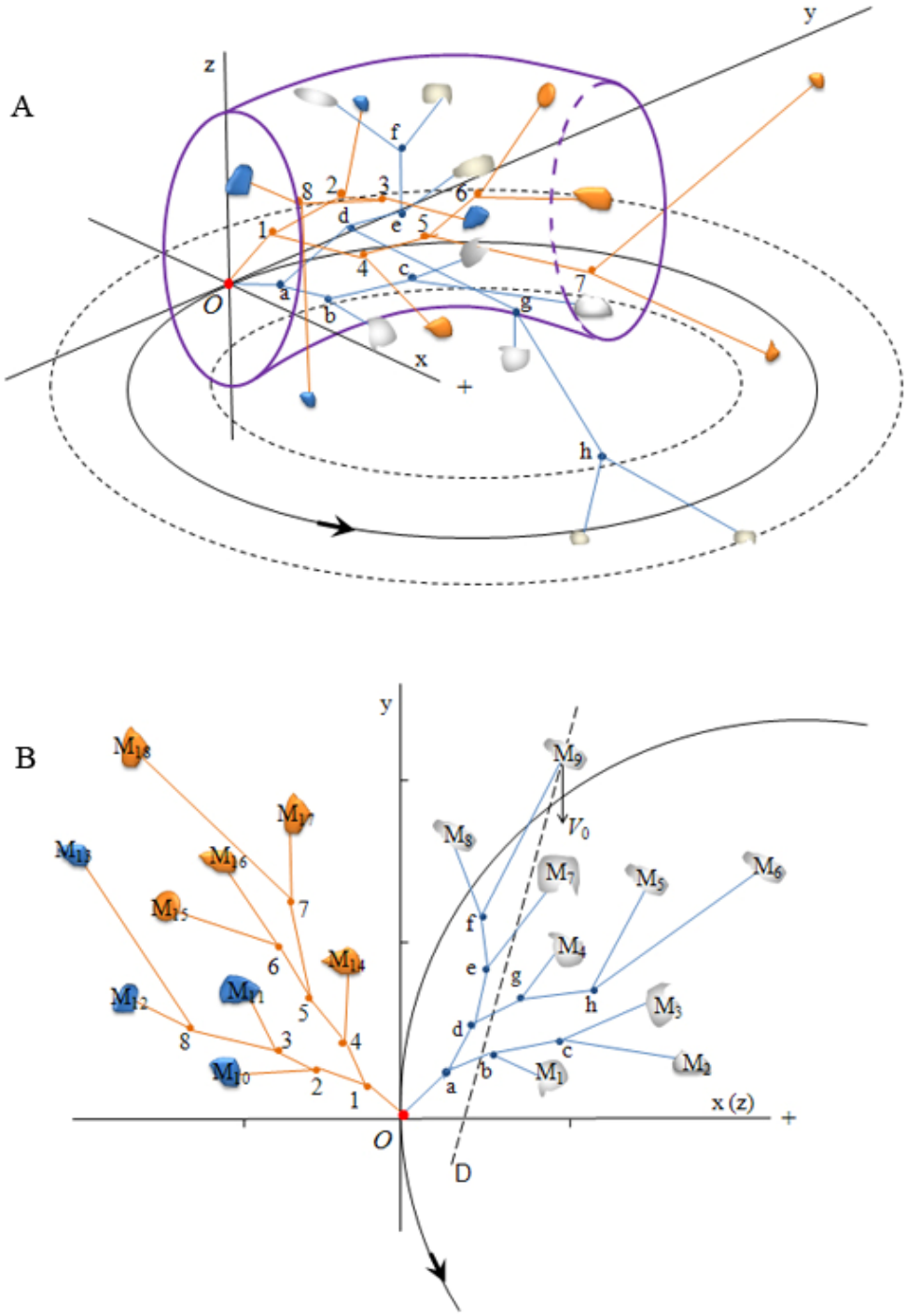

Figure 4: Fragment's modeling arrangement A: fragments are being organized into a series of hierarchical two-body systems to orbit. Point *O* is the barycenter that is survived in the collision. *xoy* plane is approximately parallel to the ecliptic, while *zoy* plane is vertical to the ecliptic. Curved cylinder represents a spatial distribution of fragments; B: four branches of fragments are ideally assigned at *xoy*, *-xoy*, *zoy*, and *-zoy* plane, respectively. Note each branch here represents two. *y* axis is

always tangential to the orbit of the barycenter (point *O*).

The result shows that the fragments under the effect of a series of hierarchical two-body confinements run a very lengthy falling, by which they gradually fall into a circular belt around the Sun. Specifically speaking, in the direction of *z* axis that is approximately vertical to the ecliptic, after a time of 3.9 billion years 83% the sample fragments fall into a distance of less than 0.15 AU from the ecliptic. With the passage of time, the belt is confined to vertically become thinner and thinner. Contrary to this, in the direction of *x* axis that is always directed towards the Sun, during a time of 2.3 billion years these fragments are always approaching the orbit of the barycenter (point *O*), by which the belt is radially confined (the least width of the belt is around 0.56 AU), but when the right branch of fragments M_1~M_9 ride over the orbit of the barycenter (point *O*), the radial velocity difference between these fragments and barycenters can lead the belt to radially spread out, by which the belt becomes wider and wider, even if these fragments are always approaching the orbit of the barycenter (point *O*). The longitudinal velocity difference between these fragments can also lead them to spread out, by which the belt is stretched into a full circle around the Sun. The time for forming such a circle may be expressed as

$$t = \frac{2\pi}{\left(\frac{\sqrt{{V_1}^2+(a_1 t)^2-2\times V_1\times a_1 t\times\cos\alpha_1}}{\mathrm{R_1}} - \frac{\sqrt{{V_2}^2+(a_2 t)^2-2\times V_2\times a_2 t\times\cos\alpha_2}}{\mathrm{R_2}}\right)}$$ (where V_1 and V_2 are respectively the initial velocity of two fragments, a_1 and a_2 respectively their acceleration, α_1 and α_2 respectively the angle between the tangential velocity and gravitation, $\mathrm{R_1}$ and $\mathrm{R_2}$ the orbital radius, note that each fragment is approximately taking a velocity of *V* to run a circle of radius R around the Sun). According to Figure 4 and Table 2, in the left branch of fragments $L_{O\text{-M14}}$ = 0.263 AU, while $L_{O\text{-M18}}$ = 0.738 AU, the two are respectively the nearest and most distant, fragment M_{14} is therefore the fastest to longitudinally catch up with fragment M_{18} than other fragments. The time for the circle's formation is worked out to be 91.51 years on the assumptions that $a_1 = \bar{a} \times (\frac{\mathrm{R}}{L_{\mathrm{Sun-M14}}})^2$, $a_2 = \bar{a} \times (\frac{\mathrm{R}}{L_{\mathrm{Sun-M18}}})^2$, $\alpha_1 = \alpha_2 = 20°$.

Observation shows that the major part of the asteroid belt is from 2.15 to 3.3 AU. In this simulation, the 18 sample fragments are initially assigned at a range of less than 0.8 AU from the collisional origin (the origin at the moment is at a distance of 4.13 AU from the Sun), they at present form a belt of only 2.77 AU ~ 3.45 AU from the Sun. This suggests that the distance of the

origin and the Sun we empirically estimated is too much, if this distance is reduced by 0.3 AU, the result will match the observation very well. It is necessary to note that the number of sample fragments selected here is far less than the real value of the fragments that are ejected from the collision of the binary planetary system. Moreover, all fragments are randomly ejected from the collisional origin and then are spherically distributed around it, the fragments in Figure 4(B) are only the representatives of all fragments. In practice, the majority of the fragments are distributed neither in the *xoy* plane nor in the *zoy* plane, instead, they are distributed freely between the four branches of fragments. But anyway, such a hierarchical two-body confining configuration may effectively reflect the formation of the whole asteroid belt.

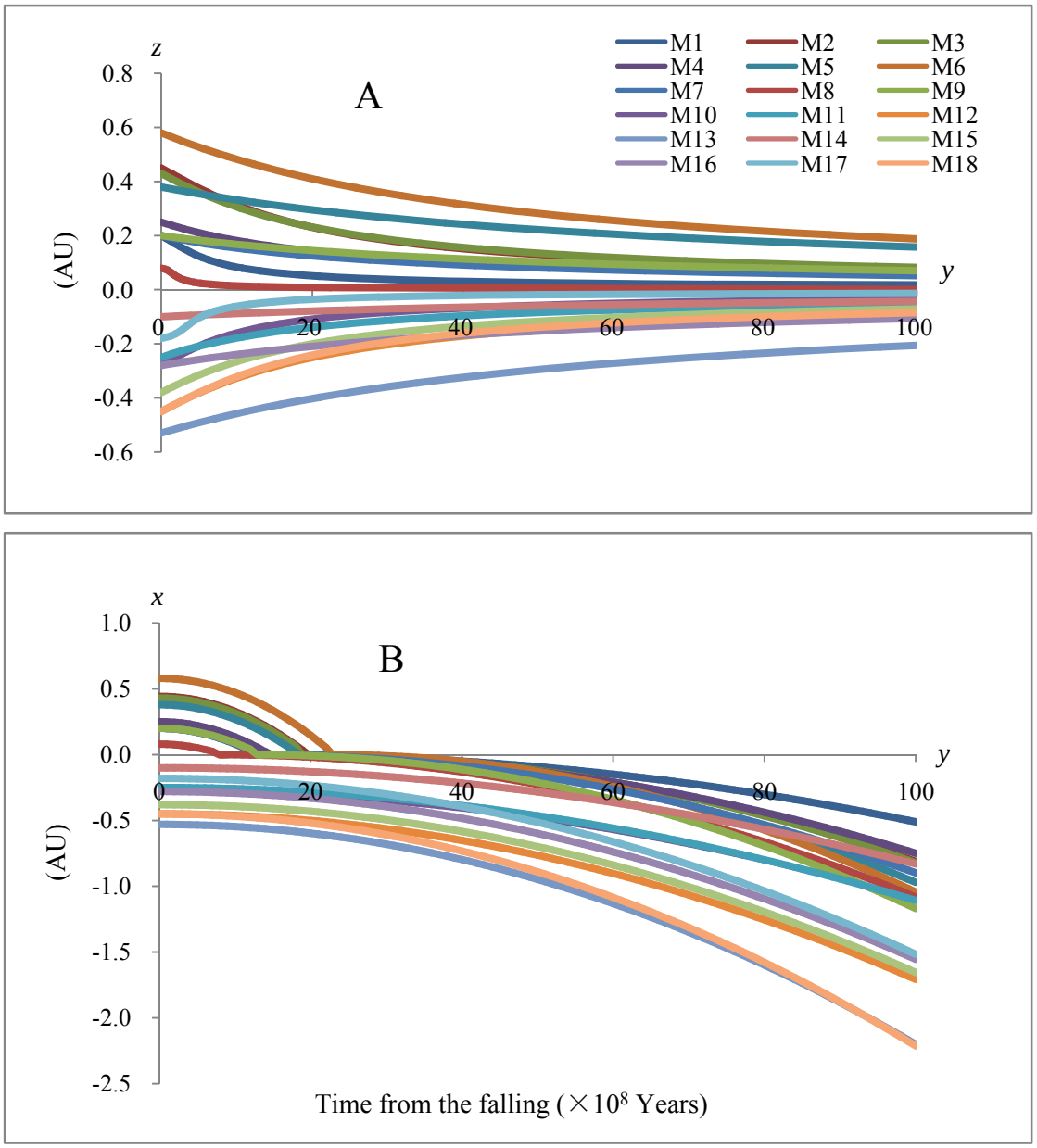

Figure 5: Fragment's motion out to time. A: fragments are vertially falling on *xoy* plane that is

parallel to the ecliptic; B: fragments are radially approaching the orbit of the barycenter (point *O*) that is always tangential to *y* axis. The present is at the time of 3.9 billion years.

Barycenter and fragment	Coordinate		Mass (*m*)
	x(z)	y	
O	0.00	0.00	1.00
a	0.08	0.08	0.30
b	0.15	0.10	0.15
c	0.25	0.11	0.05
d	0.10	0.13	0.15
e	0.13	0.20	0.07
f	0.13	0.28	0.03
g	0.18	0.15	0.08
h	0.30	0.16	0.04
1	0.05	0.05	0.70
2	0.13	0.08	0.57
3	0.20	0.11	0.27
4	0.10	0.11	0.13
5	0.15	0.18	0.11
6	0.23	0.25	0.04
7	0.21	0.33	0.07
8	0.35	0.13	0.07
M_1	0.20	0.08	0.10
M_2	0.45	0.10	0.03
M_3	0.43	0.15	0.02
M_4	0.25	0.25	0.04
M_5	0.38	0.35	0.03
M_6	0.58	0.38	0.01
M_7	0.20	0.38	0.02
M_8	0.08	0.43	0.01
M_9	0.20	0.55	0.04
M_{10}	-0.28	0.08	0.30
M_{11}	-0.25	0.18	0.20
M_{12}	-0.45	0.15	0.03
M_{13}	-0.53	0.38	0.04

M_{14}	-0.10	0.23	0.02
M_{15}	-0.38	0.30	0.03
M_{16}	-0.28	0.40	0.01
M_{17}	-0.18	0.45	0.06
M_{18}	-0.45	0.58	0.01

Table 1: Parameter assignment of fragments (barycenters) in the model. 1m = 70% the mass of the binary planetary (satellite) system.

It can be inferred that under the frame of hierarchical two-body association, every fragment will have a companion that is either a fragment or an association of a series of subordinate hierarchical two-body systems of small fragments. The fragment and its companion naturally may form a binary system in space. This point has been partially proved that because nearly all of the solar system's small-body reservoirs have been found to hold binaries (Funato et al. 2004; Durda et al. 2006; Weidenschilling, 2002; Goldreich et al. 2002; Astakhov et al. 2005; Canup 2005). Recent surveys discovered that ~16% of near-Earth asteroids, ~2% of large main-belt asteroids, and ~11% of Kuiper-belt objects are being orbited by satellites (Margot et al. 2002; Merline et al. 2002; Stephens and Noll 2006). A smashing collision of the two bodies of a previous binary planetary system is competent. The resemblance of chemical composition between the binary planetary system and the Earth-Moon system unquestionably may account for the diversity of chemical composition between the asteroids. After the disruption, the melting materials stored in the bodies of the binary planetary system may be released and recrystallized due to a change of temperature and pressure. The asteroids are currently observed to be with an irregularly but smooth appearance, this may be explained as the sharp fragments ejected had been long-termed erode by the interstellar dust. Estimate of shattering energy for the binary planetary system follows this process. Due to M_{Earth}= 5.97×10^{24} kg, M_{Moon}= 7.35×10^{22} kg, $L_{\text{Earth-Moon}}$ = 384 000 km, P_{Moon} = 27.32 days, R_{Earth} = 6 370 km, R_{Moon} = 1 738 km (where M_{Earth} and M_{Moon} are respectively the mass of the Earth and Moon, $L_{\text{Earth-Moon}}$ is the distance between the Earth and Moon, P_{Moon} is the orbital period of the Moon, R_{Earth} and R_{Moon} are respectively the radius of the Earth and Moon), thus the orbital radius of the Moon in the Earth-Moon system is L_{Moon} = (M_{Earth}×$L_{\text{Earth-Moon}}$)/(M_{Earth}+ M_{Moon}) =379 330 km, the orbital velocity is V_{Moon} = 2πL_{Moon}/ P_{Moon} =

1.0 km s^{-1}, the orbital radius of the Earth in the Earth-Moon system will be $L_{Earth} = L_{Earth\text{-}Moon} - L_{Moon}$ = 4 670 km, the orbital velocity is $V_{Earth} = L_{Earth} \times V_{Moon} / L_{Moon}$ = 0.012 km s^{-1}. The kinetic energy for the Earth-Moon system will be $E_k = (M_{Earth} \times V_{Earth}^2 + M_{Moon} \times V_{Moon}^2)/2 = 3.72 \times 10^{28}$ J. When the Moon collides with the Earth, their gravitational potential is converted to kinetic energy, thus $E_p = GM_{Earth}M_{Moon}[(1/L_{Moon1} - 1/L_{Moon2}) + (1/L_{Earth1} - 1/L_{Earth2})]$ (where L_{Eoon1} is the gravitational distance of the Moon to the barycenter of Earth-Moon system when the collision occurs, L_{Moon2} the initial gravitational distance, L_{Earth1} the gravitational distance of the Earth to the barycenter of Earth-Moon system when the collision occurs, L_{Earth2} the initial gravitational distance. After a deduction, L_{Moon1}= 8 009 km, L_{Moon2} = 379 330 km, L_{Earth1}= 98 km, L_{Earth2}= 4 670 km), thus the gravitational potential work is worked out to be $E_p = 2.93 \times 10^{32}$ J. Also note that in the frame of hierarchical two-body system the Sun and other planets are exerting gravitation to the Earth and Moon by means of the barycenters of a series of hierarchical two-body systems, but at a large distance other planet's effect on the Earth and Moon may be overlooked. As a result, the Sun's gravitational work to the Earth and Moon is $E_{Sun} = GM_{Sun} \times [M_{Moon}(1/L_{Moon\text{-}Sun1} - 1/L_{Moon\text{-}Sun2}) + M_{Earth}(1/L_{Earth\text{-}Sun1} - 1/L_{Earth\text{-}Sun2})] = 3.23 \times 10^{29}$ J, where $G = 6.67 \times 10^{-11}$ m^3 kg^{-1} s^{-2}, $M_{Sun} = 1.9891 \times 10^{30}$ kg, $L_{Moon\text{-}Sun1}$ is the gravitational distance of the Moon to the Sun (that is equal to $L_{Moon1} + L_{bary\text{-}Sun} \approx 8\ 009 + 149\ 598\ 000 = 149\ 606\ 009$ km) when the collision occurs, $L_{Moon\text{-}Sun2}$ the initial gravitational distance (that is equal to $L_{Moon2} + L_{bary\text{-}Sun} \approx 379\ 330 + 149\ 598\ 000 = 149\ 977\ 330$ km), $L_{Earth\text{-}Sun1}$ the gravitational distance of the Earth to the Sun (that is equal to $L_{Earth1} + L_{bary\text{-}Sun} \approx 98 + 149\ 598\ 000 = 149\ 598\ 098$ km) when the collision occurs, $L_{Earth\text{-}Sun2}$ the initial gravitational distance (that is equal to $L_{Earth2} + L_{bary\text{-}Sun} \approx 4\ 670 + 149\ 598\ 000 = 149\ 602\ 670$ km). The total energy for the Earth-Moon system at the moment when the collision occurs will be $E = E_k + E_p + E_{sun} \approx 2.93 \times 10^{32}$ J (we assumed that the collision occurs at the moment when $L_{earth\text{-}moon} = R_{earth} + R_{moon}$ = 8 108 km). Such a quantity of energy is powerful enough to shatter the two bodies of the binary planetary system into small fragments.

3.2 Planetary ring

Observation shows that the rings of each giant planet are mutually parallel and there are many divisions within them. For example, Cassini division, Roche division, and so on are in the Saturn's rings, the voids between the rings of Uranus and Neptune may be treated as divisions. These divisions look like natural boundaries, but the particles in each ring do not ride over them.

A broad, flat profile is very common in the rings of four giant planets' rings, for example, the Jupiter's rings, the Saturn's rings, Uranus's 1986U2R/ζ, ν and μ rings, and the Neptune's Galle, and Lassell rings. Many irregularly shaped satellites have been found within (or in) the planetary rings. For example, Adrastea and Metis are embedded in the Jupiter's main ring, while Amalthea is embedded in the Gossamer ring. Mimas, Enceladus, and Tethys are embedded in the Saturn's E ring. Cordelia, Ophelia, Bianca, Cressida, Desdemona, Portia, Rosalind, Cupid, Belinda, Perdita, and Puck are embedded within (or in) the Uranus's rings. Naiad, Thalassa, Despina, Galatea, and Larissa are within the Neptune's rings. The structure of moonlet and clump has also been detected in the rings (Esposito et al. 2008). It has been observed that the Saturn's rings have different spectral characteristics. Figure 6 shows the appearances of several giant planet ring systems.

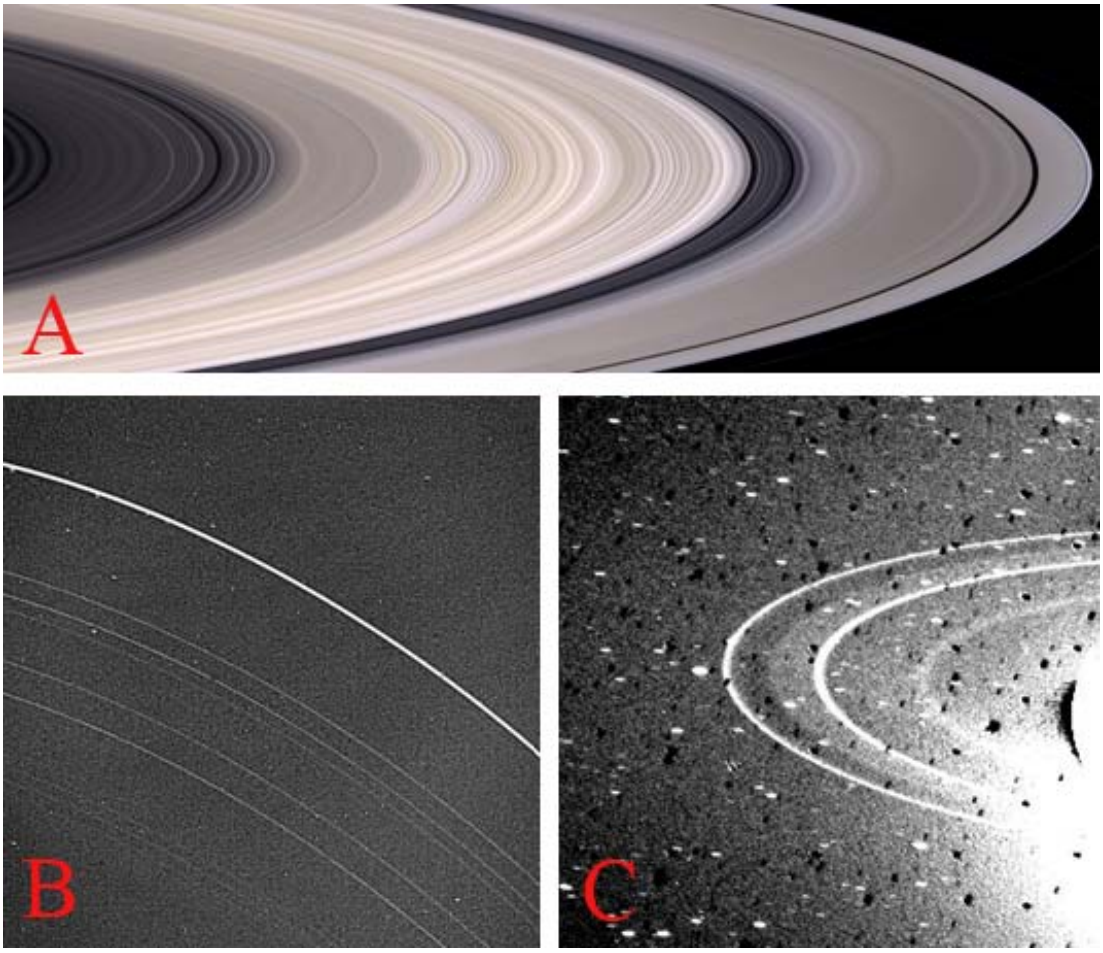

Figure 6: General view of several giant planet's ring systems. A: Saturn Rings taken 12 December 2004; **B**: Voyager 2 picture of Uranus' rings taken on 22 January 1986; **C**: Voyager 2 picture of Neptune's rings taken on 26 August 1989. Credit: NASA/JPL/Space Science Institute.

Reference to Figure 1, it can be inferred that some of the fragments may be further shattered into very small fragments (particles with a size of meter or micron, for instance) that are still organized in a series of hierarchical two-body systems. With the passage of time, the longitudinal velocity difference between these small fragments that are from a common parent body will lead them to stretch and eventually form a full belt (ring) around the center body. The disruptions of many fragments may thus form many full belts (rings) around the center body. The non-disrupted fragments are left to be embedded in (within) the belts (rings) to orbit together, by which they are called shepherds. Given the orbital decrease as proposed (Yang 2011), the survived barycenter will drag these belts (rings) of fragments to radially immigrate towards the center body, the radial velocity difference will make the belts (rings) slowly become flat. As the fragments are separated in space, there must form divisions between the belts (rings) when they are disrupted. Also because the particles of each ring are confined by the barycenters of a series of hierarchical two-body systems to orbit, the parallel, independent rings are determined. As the two bodies of the binary satellite system are composed of different materials, different fragments ejected may hold different proportional materials, and then, when they are further shattered into very small fragments to form belts (rings), different spectral characteristics are determined for the belts (rings). Reference to Figure 4, the fragments distributed at the *xoy* plane can make only radial immigration, while the fragments distributed at the *zoy* plane can make not only radial immigration but also vertical falling, this means that the distribution of different material fragments may be finally crossbedded. However, if a fragment is disrupted not in depth, the remaining may be embedded in the particles of the ring to create the structure of moonlet and clump. Figure 7 demonstrates an artistic configuration of planetary ring systems, in which all fragments (particles) are being organized in a series of hierarchical two-body systems to orbit.

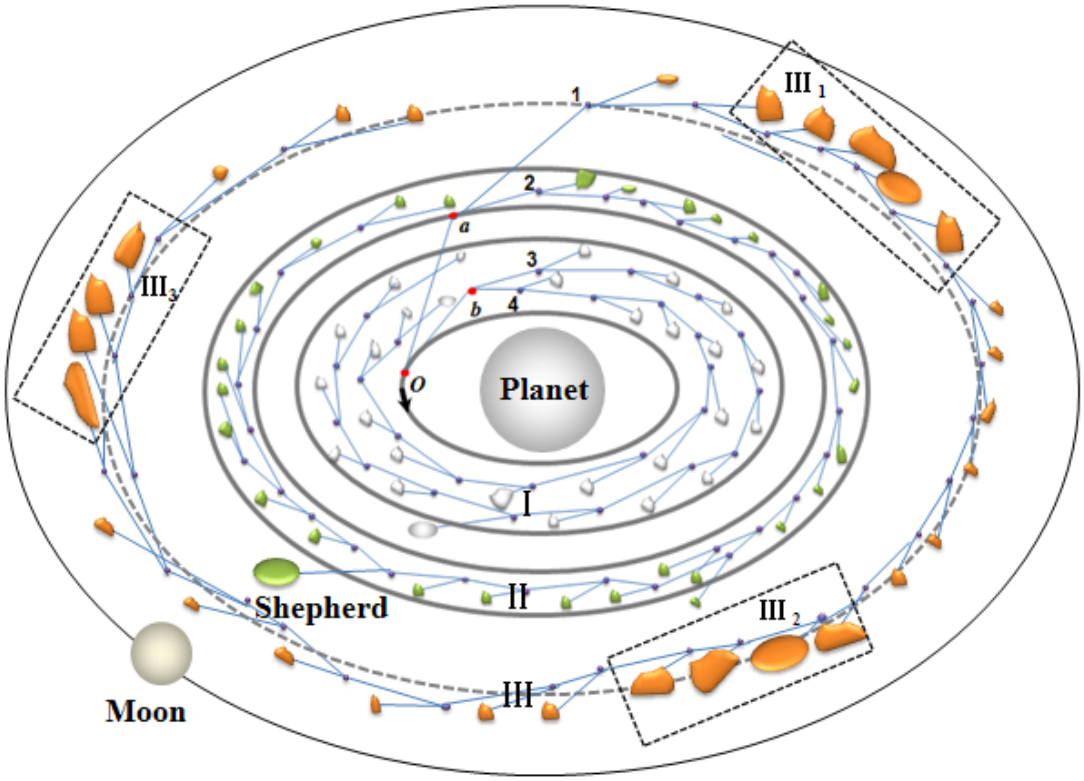

Figure 7: A hierarchical two-body association of fragments (particles) for planetary ring system. Planet is equivalent to Jupiter, Saturn, Uranus, and Neptune, respectively; Ⅰ is equivalent to planet's broad rings like Gossamer rings of Jupiter, A, B, C, D, and E rings of Saturn; Ⅱ is equivalent to planet's general rings like Janus/Epimetheus, G, and Pallene rings of Saturn, 1986U2R/ζ and μ rings of Uranus, Lassell ring of Neptune; Ⅲ is equivalent to planet's narrow rings like F ring of Saturn, 6, 5, 4, α, β, η, γ, δ, λ, ε, ν rings of Uranus, Galle, Le Verrier, and Adams rings of Neptune; $Ⅰ_1$, $Ⅱ_2$, and $Ⅲ_3$ is equivalent to ring arcs (clumps) like Methone and Anthe arcs of Saturn, Fraternité, Égalité 1, Égalité 2, Liberté, and Courage arcs of Neptune. Any two adjacent rings are naturally divided by gap (division). Point *O* is the barycenter of integral ring system that drags point *a* and *b* to orbit the planet, at the same time point *a* drags point 1 and 2 to orbit, point *b* drags point 3 and 4 to orbit, while point 1, 2, 3, and 4 respectively drags a series of hierarchical two-body associations of fragments to orbit, by which several rings are formed around the planet. Red (brown) dot denotes the barycenter of related two-body system, blue line denotes gravitation. Large black arrow denotes the mean motion of integral ring system. Different color in the ring system denotes different chemical composition.

We use the parameters in Figure 4 and Table 1 to quantify the formation of the Saturn's ring

system. The center body is replaced with the Saturn. The coordinate unit is million kilometers. As the Sun's gravitation to planet is different from planet's gravitation to satellite, the relation of acceleration and gravitation for satellite needs to be recalculated. Similarly, the orbital decreasing rate for the Moon was $\Delta \mathrm{R}_{\mathrm{Moon}} = 4.4583 \times 10^{-7} \times t + \frac{1}{2} \times 3.071 \times 10^{-18} \times t^2$ km (where the unit of t is in days). Given the relation of acceleration and gravitation for the Moon may be expressed as $\Delta \mathrm{R}_{\mathrm{Moon}} \sim \frac{GM_{\mathrm{Earth}}}{L_{\mathrm{Earth-Moon}}{}^2}$, which is applicable for any planet and its satellite, the orbital decreasing rate for the binary satellite system may thus be written as

$$\Delta \mathrm{R}_{\mathrm{o}} = \frac{M_{\mathrm{Saturn}}}{M_{\mathrm{Earth}}} \times \left(\frac{L_{\mathrm{Earth-Moon}}}{L_{\mathrm{Saturn-o}}}\right)^2 \times \Delta \mathrm{R}_{\mathrm{Moon}} = 13.74 \times (4.4583 \times 10^{-7} \times t + \frac{1}{2} \times 3.071 \times 10^{-18} \times t^2)$$

if $L_{\mathrm{Saturn\text{-}O}}$ is assumed to be 1 000 000 kilometers (where M_{Earth} = 5.97×10^{24} kg, M_{Saturn} = 5.68×10^{26} kg, $L_{\mathrm{Eartg\text{-}Moon}}$=380 000 km). We further define $\Delta \mathrm{R}_{\mathrm{O}} = \bar{a}t$ to obtain an average acceleration for the binary satellite system. Given all fragments are constrained by the same gravitation origin-the Saturn, the acceleration for each fragment may be further expressed as $a = \bar{a} \times \left(\frac{L_{\mathrm{Saturn-o}}}{L_{\mathrm{Saturn-fragment}}}\right)^2$. Initial velocity for fragment is assumed to be $V_0 = \sqrt{\frac{GM_{\mathrm{Saturn}}}{L_{\mathrm{Saturn-fragment}}}}$ (where gravitational constant G = 6.67×10^{-11} $\mathrm{m^3\ kg^{-1}\ s^{-2}}$, the Saturn's mass M_{Saturn} = 5.68×10^{26} kg, $L_{\mathrm{Saturn\text{-}fragment}}$ is the distance of a fragment and the Saturn).The Saturn's gravitation to the binary satellite system here is thought to be primary. We further assumed that the majority of the fragments are disrupted into very small fragments (the size of water particles, for example) that are still organized in a series of hierarchical two-body systems to from the rings. As shown in Figure 8 and 9, the fragments in the direction of *z* axis run a very lengthy falling, during a period of 2 billion years, they generally fall into a distance of less than 10 000 km from *xoy* plane (that is approximately parallel to the Saturn's equatorial plane), some of them may even reach a distance of less than several kilometers. In the direction of *x* axis (that is directed towards the Saturn) the right branch of fragments (M_1~M_9, for example) take a time of approximately 180 million years to reach the orbit of the barycenter (point *O*), during this period the left branch of fragments (M_{10}~M_{18}, for example) due to radial velocity difference are slowly departing from the orbit of the barycenter (point *O*), even though all fragments and barycenters are approaching the planet forever. Around 300 million years later, the orbit of the barycenter (point *O*) immigrates to a distance of 137 000 km from the planet, the width of all fragments varies from 1

110 000 to 1 040 000 million kilometers. Among of them, the nearest fragment (M_2) is at a distance of 137 000 km from the planet, while the furthermost fragment (M_{13}) is 1 230 000 km from the planet. The vertical falling and radial immigration together make the belt of fragments become flat. As the binary satellite system is composed of mainly ice + silicate + oxygen, ice rings may thus be determined. Unlike the fragments of the binary planetary system that are responsible for the asteroid belt, every fragment here may form an independent ring when disrupted. Unfortunately, the time for disrupting a fragment is unknown, the timescale of forming a full ring is hard to quantify. The mass and disruptive severity of a fragment controls the width of a ring that forms from it, but it cannot be quantified here, too. But the creation of a ring may be roughly expressed by Figure 4 (B) that a moving fragment due to disruption creates a configuration of the left branch of fragments (M_{10}-$M_{18,}$ for instance) that are still organized in a series of hierarchical two-body systems, the longitudinal velocity difference between these fragments leads them to stretch and forms a full ring, while the radial velocity difference leads them to spread out and makes the ring flat. The simulation also reflects a fact that the vertical falling relative to radial immigration is too slow. This requests that the binary satellite system is at a distance of far larger than 1 000 000 kilometers from the Saturn when the collision takes place. The distance must be large enough for the barycenter of the binary satellite system to fall during a time of billions of years. Table 2 shows a radial timescale for the formation of the Saturn's rings.

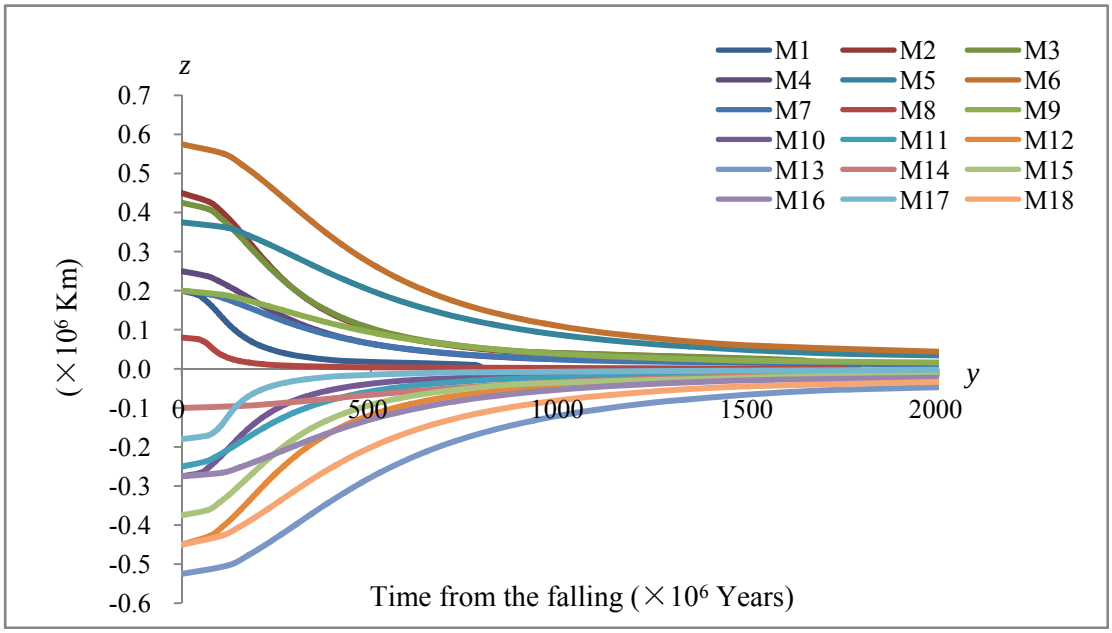

Figure 8: Fragment's vertical confinement. All fragments distributed in the direction of *z* axis are slowly falling on *xoy* plane that is parallel to the Saturn's equatorial plane, by which the rings become

thinner and thinner.

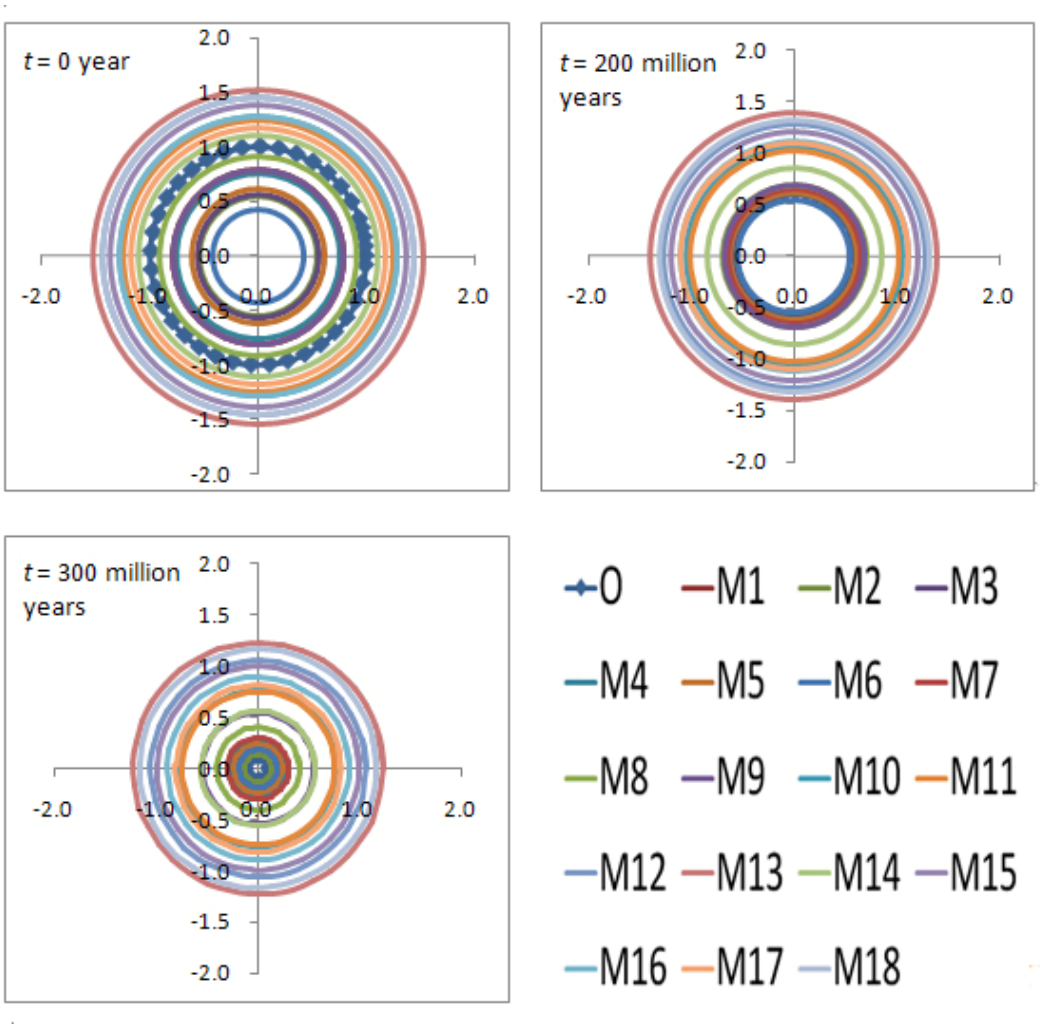

Figure 9: Evolution of fragment's orbit. The Saturn is at the center of the coordinate frame. The unit of the coordinate axis is million kilometers. Note that some of the fragments can be further shattered into small fragments to form independent rings, thus the orbit of each fragments may represent the orbit of a ring.

Ring name	Distance from Saturn's center (km)	Width (km)	Ro (km)	$L_{M14\text{-}M18}$	Time ($\times 10^6$ years)
D	66,900 – 74,510	7,500	66,900	350	704
C	74,658 – 92,000	17,500	74,658	350	1,327
B	92,000 – 117,580	25,500	92,000	350	1,889
A	122,170 – 136,775	14,600	122,170	350	1,592
G	166,000 – 175,000	9,000	166,000	350	1,414

Table 2: Radial formation timescale for the Saturn's rings. Assumed that the barycenter (point *O*) of the binary satellite system is now located at the inner edge of D ring, its distance from the Saturn is 66 900 km, which corresponds to an orbital decreasing rate of $\triangle$Ro=13.74×$(4.4583\times10^{-7}\times t+0.5\times3.071\times10^{-18}\times t^2)$, where the unit of *t* is in days. Every ring is derived from the disruption of a fragment and is closely controlled by a leading subordinate barycenter that is also located at the inner edge of the ring. The plant indirectly controls the particles of each ring through the barycenter (point *O*), the leading subordinate barycenter, and the barycenters of a series of interior hierarchical two-body systems. The particle assignment in the ring is similar to the configuration of the left branch of fragments in Figure 4(B). The coordinate unit in Table 1 is defined as 1000 km. M_{14} and M_{18} (relative to the planet) are considered to be respectively the nearest and furthermost two particles in the ring. The orbital decreasing rate for each particle may be further expressed as $\triangle R_M = (L_{\text{Saturn-fragment}}/L_{\text{Saturn-o}})^2 \times \triangle$Ro (where $L_{\text{Saturn-o}}$ represents the distance of the planet and the barycenter (point *O*), $L_{\text{Saturn-fragment}}$ the distance of the planet and the fragment, which is equal to the sum of the distance of leading subordinate barycenter to the planet and the distance of leading subordinate barycenter to the particle). The radial times for a ring's formation may thus be determined through a relation of $L_{\text{ring}} - L_{\text{M14-M18}} = (\Delta R_{M14} - \Delta R_{M18}) \times \sin\alpha$, where L_{ring} is the width of a ring, $L_{\text{M14-M18}}$ the initial radial distance between the two particles, α the angle between the tangential velocity and gravitation, which is assumed to be identical for the two particles and here is defined as 10^o.

The propeller-shaped and ringlet structures in the Saturn's ring and the twisted Fraternity arc in the Neptune's ring may be explained as follows (Fig.10): because the two bodies of a two-body system are derived from the disruption of a common parent body, after the disruption the two run parabolic trajectories around their barycenter (proper motion), but because the barycenter of the parent body is survived in the disruption and continues to orbit, the two bodies under the interaction of proper motion and the drag from the barycenter can display some kind of rotation in space, this makes them look like a two-armed propeller if they are embedded in the particles of the ring. If the two bodies are further shattered to form two subordinate associations of particles, the two associations can also perform some kind of rotation, which makes them enlace with each other (like a twisted strand or rope). If only one body is shattered to form an association of

particles, while another is survived, the survived body will accompany the association to orbit together, which makes it look like a shepherd. Because of the rotation, each association of particles itself looks like a long ringlet.

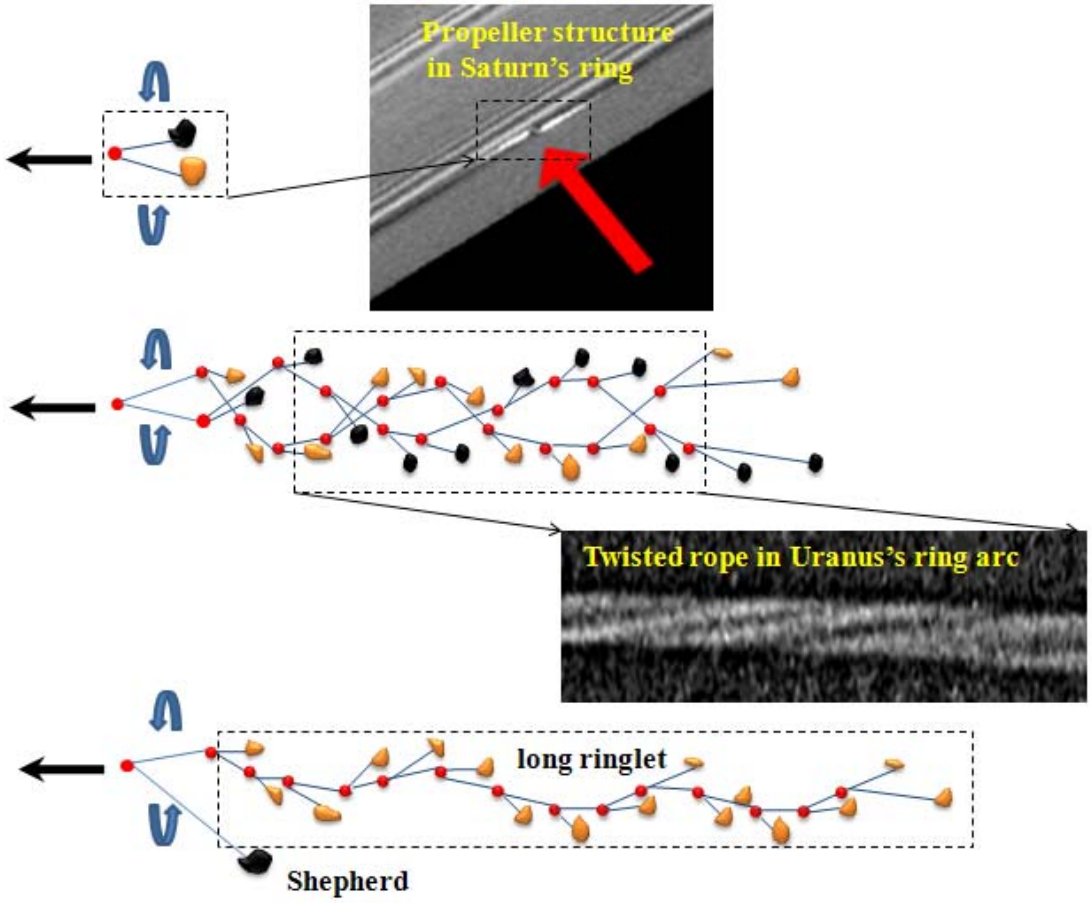

Figure 10: Model of the formation of unusual structures. Top shows a moving rotational two-body system that fits to yield a propeller structure in Saturn's ring; Middle does a moving hierarchical two-body association of particles that fits to yield a twisted strand (rope) in Uranus's Fraternity arc. Also note that in the image there are at least three hierarchical two-body associations of particles to build up this twisted rope; Bottom does a moving two-body system that consists of a shepherd (satellite) and a long ringlet (a subordinate hierarchical two-body association of particles). Red dot denotes the barycenter of related two-body system. Large black arrow denotes the motion of an integral system (images by courtesy of NASA).

Images show that Saturn's F ring has two additional strands and a background dust population that extends across ≥ 700 km in radius (Murray et al. 1997; Porco et al. 2004 and 2005), the shepherd satellite-Prometheus penetrates the inner dust region each orbital period of 14.7h,

Murray et al (2005) explained the streamer-channels as a consequence of Prometheus dragging out materials from the ring. Here please note three features: 1) the relative precession rate between Prometheus and F ring is 0.057^{o} d^{-1} (Murray et al. 2005), which indicates F ring and Prometheus are synchronously moving forward; 2) the channels relative to Prometheus (see image PIA08397) are moving backward; and 3) there are a series of channels along F ring (reference to PIA11589). Prometheus in its orbit may periodically penetrate the ring region, but it is impossible for it to drag out materials from the ring to maintain these separated longitudinal channels at the same time, unless we do not use Newton's gravity to work. Reference to Figure 7, we may employ this hierarchical two-body model to account for the formation of longitudinal channel. As the particles in F ring and the background dust region and Prometheus are being organized in a series of hierarchical two-body systems to orbit the planet, when Prometheus run a parabolic trajectory around a barycenter (proper motion) that should lie in the vicinity of F ring, it can approach and penetrates the ring region if the radius of parabolic trajectory is large enough, it firstly collides with the particles in the near side and thus pushes some of them away from the ring, the departing particles by means of the barycenters of a series of hierarchical two-body systems further drag the particles in the rear to move, by which the particles are continuously pushed away from the ring, but because the rear particles are always being dragged by the front particles to orbit, the departing particles will subsequently be dragged to return to the ring, this gives rise to an impressive effect: the particles are successively pushed away from the ring, but subsequently they are dragged to return to the ring, a wave-like appearance (look like a channel) is formed to move backward along the ring. Also because the departing particles further activate local particles, a bright feature is created for the channel. When Prometheus next time penetrates the ring region and collides with particles, another wave-like appearance (channel) is formed. Periodical collision between Prometheus and the ring region eventually yields a series of separated longitudinal channels along the ring. Figure 11 conceptually models a non-timescale collision between Prometheus and the F ring to create a channel. Prometheus has a potato-like shape (about 145 by 85 by 62 km^3), movie sequence from Cassini images (PIA08397) shows that as Prometheus approaches the F ring, it often performs some kind of rotation in space. This determines that, when Prometheus periodically collides with the elliptical F ring, the difference in collisional scale is likely to result in different size channel. Figure 12 is a reproduction of PIA08397 that records how Prometheus

interacts with F ring. It may see, when Prometheus approaches the ring (from **a** to **b,** where it is the closest approach), there is no any clue of perturbation. In other words, if there were Newton's garvity between Prometheus and the ring, Prometheus's approach will have to drag the ring to gradually become convex, but record of PIA08397 shows that before the collision the ring is always original shape, this disagrees with the expectation of Newton's gravity. It is also clear that just after the collision the F ring becomes concave (see $\mathbf{c_1}$ and $\mathbf{d_1}$).

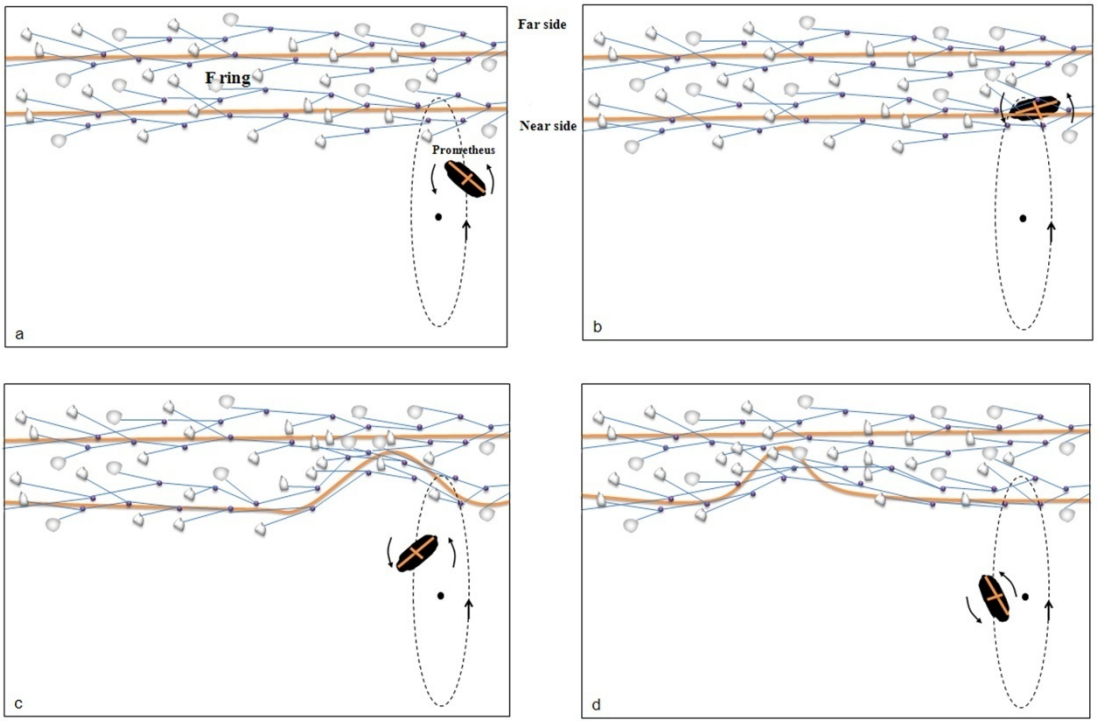

Figure 11: Modelling a channel's creation in F ring. From **a**, **b**, **c** to **d**, it succesively demonstrates how Prometeus interacts with the ring particels. Blue line denotes gravitation, the dashed circle denotes Prometheus is running a parabolic trajectyory around a barycenter (proper motion) . Prometeus and F ring are synchronaly moving towards right.

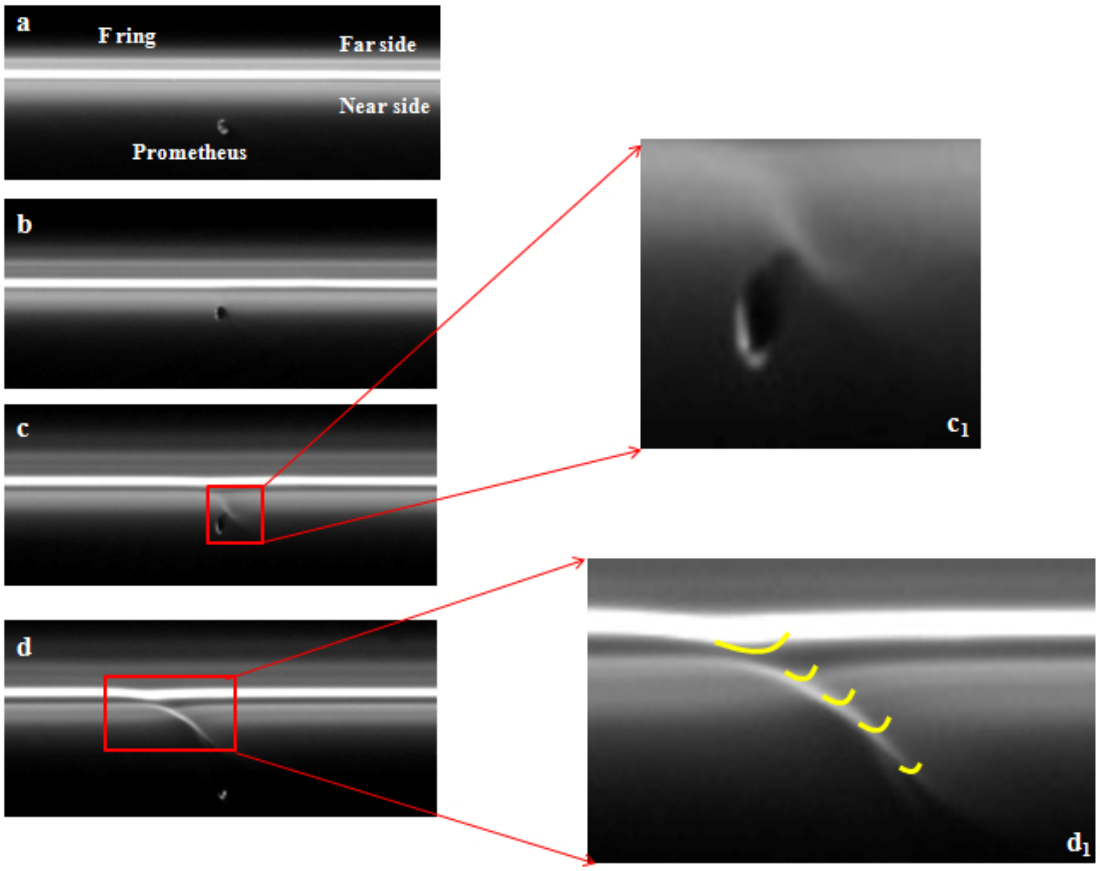

Figure 12: Cassini-Huygens's images of the interaction of Prometheus and the F ring. $\mathbf{c_1}$ shows that the collision pushes the ring to become concave, while $\mathbf{d_1}$ does that a long concave channel is created. Note that in **b** diagram Prometheus is at the closest approach to the ring, but there is no clue of perturbation of gravitation. Image by courtesy of NASA.

3.3 Comet

Comets are observed to generally have very eccentric orbits in the sky, and their orbital periods appear to be various, ranging from a few years to hundreds of thousands of years. Their icy bodies are volatile due to the Sun's radiation. Galileo's experiment of projectile suggests that the fragments ejected from a collisional origin must run some parabolic trajectories around the origin. We may infer from Galileo's experiment that, if the projectile's speed is high enough, it may circle around the Earth, if the speed is very high, it will run a very big parabolic trajectory to circle around the Earth, but anyway, the projectile due to the pull of the Earth's gravitation will eventually fall on the ground, even if it needs to take a long time to run many circles to finish this falling. This suggests that all fragments ejected from the collision of the two bodies of the binary planetary (satellite) systems will eventually fall back to the collisional origin. Reference to Figure

3, we know that every fragment is actually running a parabolic trajectory round a barycenter that is located in the asteroid belt (or planetary ring), but because of the motion of the barycenter, the parabolic trajectory will be further distorted in space. Figure 13 shows such a fragment's motion.

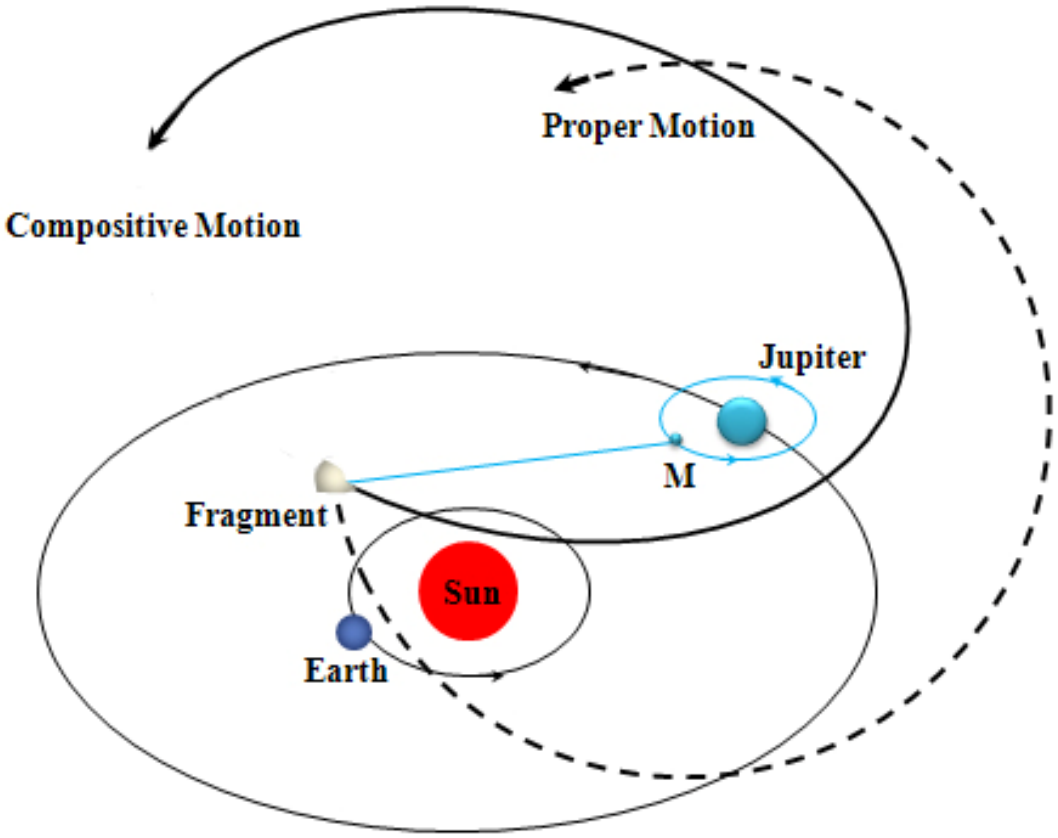

Figure 13: Motion of a fragment dominated by the Jupiter. The fragment actually is gravitationally constrained by a barycenter that is located in the Jupiter's ring system. Proper motion denotes fragment itself is running a parabolic trajectory around a barycenter (M) in the Jupiter's ring, while compositive motion denotes the proper motion due to the motion of the Jupiter around the Sun is distorted in space. Real and dashed lines denote the trajectories of related bodies.

Figure 14 shows that the fragments dominated by the asteroid belt and four giant planetary ring systems cover the solar system extensively. Reference to Figure 13, when these fragments run some parabolic trajectories around the barycenters that are located in the asteroid belt and giant planetary ring systems, they are at the same time being brought by the motions of the asteroid belt around the Sun and giant planets around the Sun to move. This makes the trajectories of all fragments distorted. Once some of these fragments approach the Sun enough, the Sun's radiation

can warm them to become comets. Do not forget a precondition that the chemical composition of the binary planetary system is similar to that of the Earth-Moon system, and the chemical composition of four binary satellite systems is also similar to that of the icy satellites of the planets, this means that the fragments ejected from these binary systems may hold water composition.

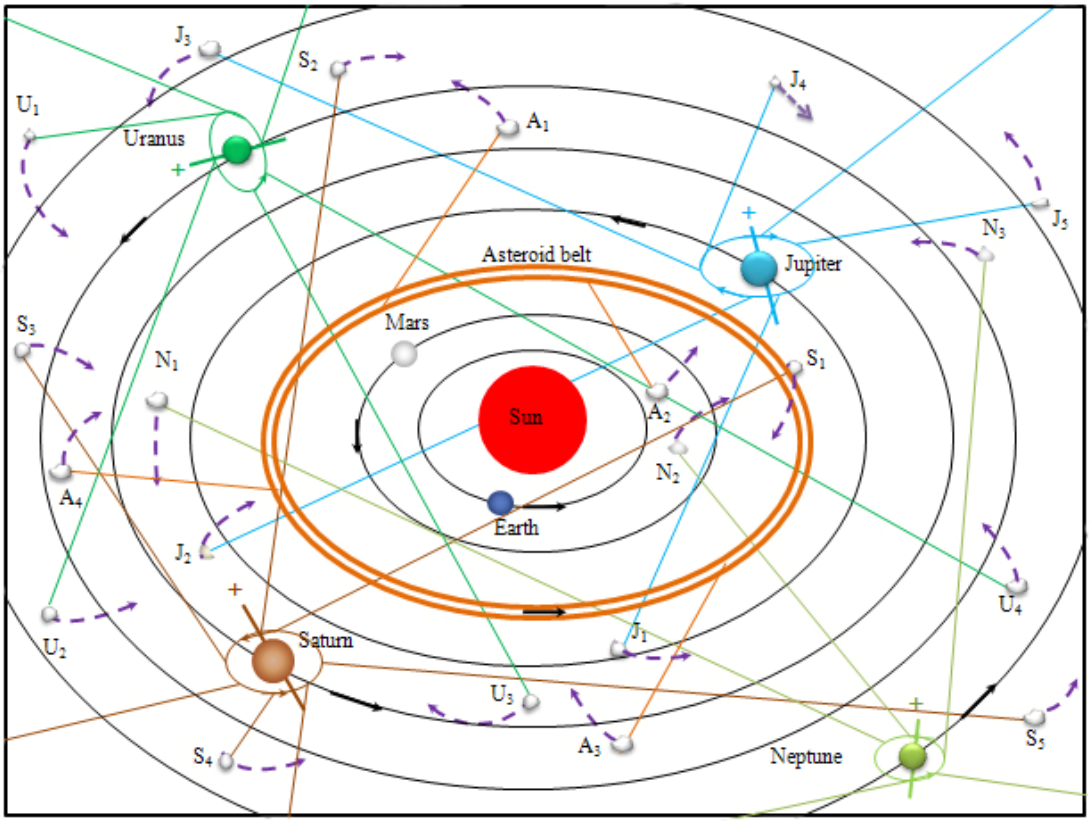

Figure 14: Motions of the fragments constrained by the asteroid belt and four giant planets. The motion of each fragment is actually constrained by a barycenter that is located either in the asteroid belt or in the planetary ring. Letter $A_{1,2,3,etc}$ ($J_{1,2,3,etc}$, $S_{1,2,3,etc}$, $U_{1,2,3,etc}$, $N_{1,2,3,etc}$) respectively denote the fragments dominated by the asteroid and four giant planetary ring systems. Various colors of straight lines represent gravitational forces from the asteroid belt and four planetary rings to fragments. "+" denotes the north pole of the planet. Arrows denote the motional directions of fragments, planets, rings, and asteroid belt in the space. Note that each fragment is running a parabolic trajectory around a barycenter that is located in the asteroid belt (or giant planetary ring), but at the same time this motion is greatly interacted due to the motions of the asteroid belt (giant planet) around the Sun.

As the distances of the asteroid belt and Jupiter to the Sun are shorter than that of the Saturn, Uranus, and Neptune, this determines that the asteroid belt and Jupiter may drag more fragments

to approach the Sun to become comets than the Saturn, Uranus, and Neptune may do. As each fragment runs a parabolic trajectory around the barycenter in the asteroid belt (or planetary ring), this determines that the comets dominated by the asteroid belt and Jupiter should have shorter periods than those dominated by the Saturn, Uranus, and Neptune. Also because the orbital velocity of the asteroid belt and Jupiter around the Sun is quicker than that of the Saturn, Uranus, and Neptune, the parabolic trajectories of the comets dominated by the asteroid belt and Jupiter are easier to be dragged to fall on the elliptic than that of dominated by the Saturn, Uranus, and Neptune. In other words, short-period comets are likely to have less inclination (with respect to the elliptic) than long-period comets. Statistical results indicates that long period comets are generally on high-inclination orbits while short period ones are mostly on low-inclination prograde orbits (Duncan et al. 1988). But note that, because of a random ejection of fragments, the comets formed from these fragments' falling will not have a prevailing direction in the sky.

It may see a relation that the value of (aphelion – perihelion)/2 of a fragment is equal to the orbital radius of its owner (planet or asteroid belt) around the Sun. Established literature shows that the perihelion and aphelion of Encke comet are respectively 0.33 and 4.11 AU, the value of (aphelion - perihelion)/2 is equal to 1.89 AU, this is roughly close to the orbital radius of the asteroid belt (2.67 AU). The orbit of Halley comet from the Sun is between 0.586 and 35.1 AU, the value of (aphelion - perihelion)/2 is equal to 17.26 AU, this is roughly close to the orbital radius of the Uranus (19.23 AU). Encke comet and Halley comet therefore may be classified to the domination by the asteroid belt and Uranus's ring system, respectively. Reference to Figure 14, given Encke comet runs a parabolic trajectory around a barycenter that is located in the asteroid belt, the orbital radius and period of this barycenter around the Sun is 2.4 AU and 4.36 years, the orbital radius and period of Encke comet around this barycenter is 2.7 AU and 1.8 years, the inclination of this barycenter's orbit to the ecliptic is zero, the inclination of Encke comet's orbit to the ecliptic is 11.78 degrees. Observation confirms that Encke comet once reached its closest approach to the Sun on 6 August 2010. We through JPL horizon system derive the vector coordinate of Encke comet at this moment: x_{Encke} = - 0.3149 AU, y_{Encke} = 0.1290 AU, z_{Encke} = - 0.0037 AU, the coordinate origin is solar system barycenter (ssb). Because the coordinate of the barycenter is unknown, it is necessary to employ a mathematical method to work out. When Encke comet is at perihelion, its projection on the ecliptic must lie in the line of the Sun and the

barycenter. We further assumed that the distance between the projection of Encke comet and the barycenter is equal to the length of the orbital radius of Encke comet around this barycenter, therefore according to a geometry, the coordinate of the barycenter is worked out to be $x_{\text{barycenter}}$ = 2.2189 AU, $y_{\text{barycenter}}$ = - 0.9150 AU, $z_{\text{barycenter}}$ = 0.0000 AU. Based on these coordinates and related parameters, the position of Encke comet at any time may be written as

$$x_t = 2.7 \times \sqrt{(1 - [\sin(\alpha + \frac{360}{1.8}t)]^2 \times [\sin\beta]^2} \times \cos(\gamma + \frac{360}{1.8}t) + 2.4 \times \cos(\gamma + 180 + \frac{360}{4.36}t) \quad (4)$$

$$y_t = 2.7 \times \sqrt{(1 - [\sin(\alpha + \frac{360}{1.8}t)]^2 \times [\sin\beta]^2} \times \sin(\gamma + \frac{360}{1.8}t) + 2.4 \times \sin(\gamma + 180 + \frac{360}{4.36}t) \quad (5)$$

$$z_t = 2.7 \times \sin(\alpha + \frac{360}{1.8}t) \times \sin\beta \quad (6)$$

Where t is time and its unit is year, α the initial angle of Encke comet to the intersection line between its orbit and the ecliptic, β the inclination of Encke comet orbit to the ecliptic that is equal to 11.78 degrees. γ is the initial angle of its projection to the x axis.

The orbit of Encke comet is then plotted (Fig.15). It can be found that Encke comet runs a very eccentric trajectory in the space, and repeatedly crosses the orbits of Mars and Earth, and even approaches Jupiter's orbit. It is clear that, although Encke comet is defined an orbital period of 1.8 years around a barycenter, because this barycenter itself is orbiting around the Sun, the time interval between Encke comet's two closest approaches to the Sun is just 3 years. The aphelion and perihelion may reach 5.1 AU and 0.3 AU, respectively, the orbital velocity of proper motion is around 44.69 km/s. It can also be found that the comet enters the inner solar system from one corner of the sky and then drops out, but next time it enters from another corner of the sky. This performance is consistent with the established observation that Encke comet approaching the Sun has not a prevailing direction because the position of Encke comet's fan relative to the Sun is different every time (as shown in Figure 16). This irregularity of a comet's entrance may mislead people believe that it is two different comets. We make expectation that, during a short period of time (from 2010-08-06 to 2017-12-20), the comet will experience two close approaches to the Earth, one close approach to the Mars, and one close approach to the Jupiter, more detail of these approaches is 0.27 AU from the Mars on 2010 November 26, 0.64 AU from the Jupiter on 2011

August 5, 0.57 AU from the Earth on 2013 July 13, and 0.36 AU from the Earth on 2016 November 15, the two closest approaches to the Sun are 0.58 AU on 2013 August 24 and 0.41 AU on 2016 September 27, respectively.

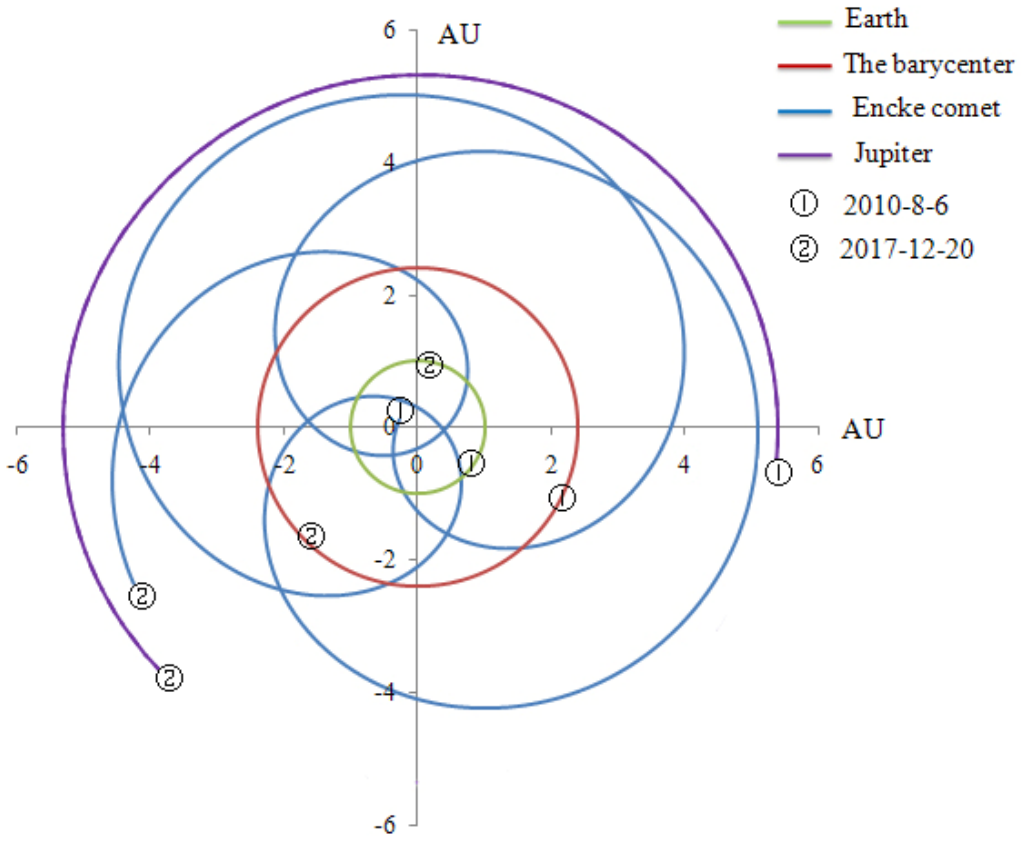

Figure 15: The orbit of Encke comet at the plane of the elliptic. The Sun is at the center. Time span is around 7 years. The coordinate origin is solar system barycenter (ssb). ① represents the position of each body on 6 August 2010, while ② the position on 20 December 2017.

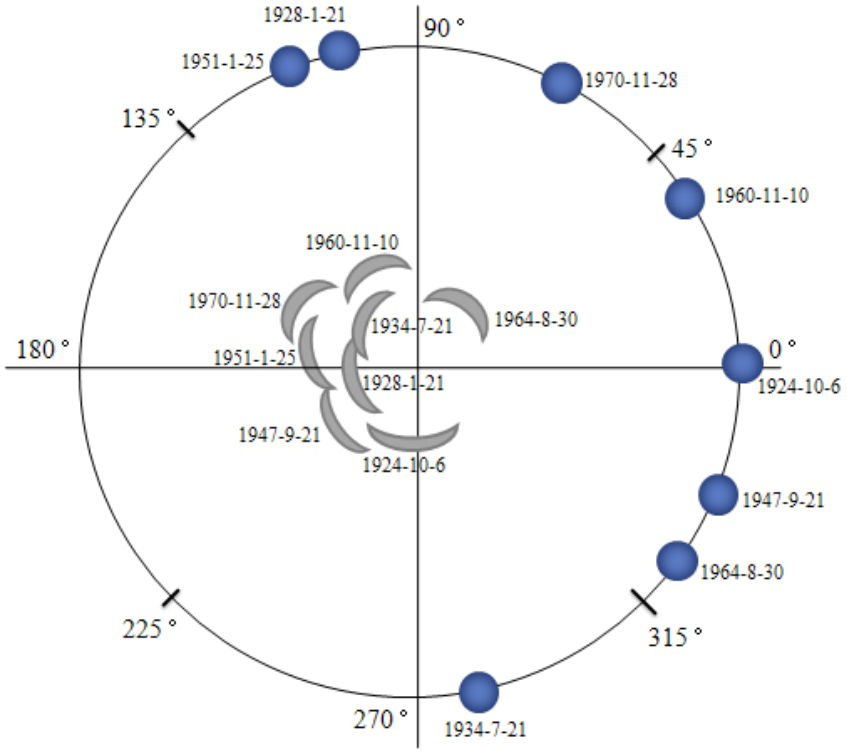

Figure 16: Relative positions of Encke comet, the Earth, and Sun during past 9 apparitions. The Sun is at the center. The data is from the work by Sekanina (1988). We firstly assumed that the Earth on 6 October 1924 is located at 0^{o}, at this moment Encke comet's fan is observed to be at the east of the Sun, and from this date to 21 January 1928 the Earth orbits around the Sun totally 1202 days that is equivalent to 3 rotations + 105.55^{o}, at this time Encke comet's fan is observed to be at the west of the Sun. Similarly, the relative positions of Encke comet, the Sun, and the Earth may be determined during past 9 apparitions.

In the past decades some small celestial bodies (they are currently named after Centaurs) had been found orbiting the Sun between Jupiter and Neptune and crossing the orbits of one or more of the giant planets (Horner et al. 2008), some of the centaurs are here classified (Tab.3). It is very important to keep in mind that a comet or centaur in the distance is very difficult to be observed because of its very small size and obscure appearance, the value of aphelion is theoretically derived from a Keplerian elliptical estimate but not from observation, and thereby has a high uncertainty to influence the precision of this classification.

Owner	Name	Perihelion (AU)	Aphelion (AU)
Jupiter	2060 Chiron	8.4	18.9

(a = 5.2AU)	1994 TA	11.7	21.9
	1995 Dw_2	18.9	31
	10370 Hylonome	18.9	31
	5145 pholus	8.7	31.8
	7066 Bessus	11.8	37.5
Saturn	1995 GO	6.8	29.4
(a = 9.3AU)	5576 Amycus	15.21	35.09
	8045 Asbolus	6.8	29.31
	7066 Nessus	11.8	37.48
Asteroid belt	1997 CU_2	13	18.5
(assumed a = 2.67 AU)	10199 Chariklo	13.08	18.66

Table 3: Classification of Centaurs. Note the values of perihelion and aphelion are derived from JPL Small-Body Database Browser, any error in these values will result in an uncertainty of this classification.

We further determine the orbit of a centaur-2060 Chiron that is constrained by the Jupiter (Fig.17). Given 2060 Chiron runs a parabolic trajectory around a barycenter that is located in the Jupiter's ring system. On a large scale, this motion may be approximately treated as 2060 Chiron is running a parabolic trajectory around the Jupiter because the ring is very close to the planet. The orbital radius and period around the Jupiter is assumed to be 13.4 AU and 6.0 years, other parameters (like orbital radius and period) of planets are derived from horizon system. It can be found that 2060 Chiron runs an eccentric orbit that is mainly located between the orbits of Saturn and Uranus, the aphelion and perihelion may reach 18.6 AU and 8.2 AU, respectively. This point is nearly consistent with the established observation. We expect, 2060 Chiron will experience one close approach from the Saturn in 2030 April (around 0.83 AU) and another approach from the Uranus in 2024 April (around 0.94 AU). Also note, any error of the positions of related bodies that we derive from horizon system will lead to an uncertainty of above expectation. It still cannot exclude a possibility that 2060 Chiron is constrained by the Saturn if the current knowledge of the

aphelion and perihelion of 2060 Chiron is not right. If so, the aphelion of 2060 Chiron must be 9.5 + 9.5 + 8.2 =27.2 AU from the Sun when the semi-axis of the Saturn is 9.5 AU and the perihelion of 2060 Chiron is 8.2 AU.

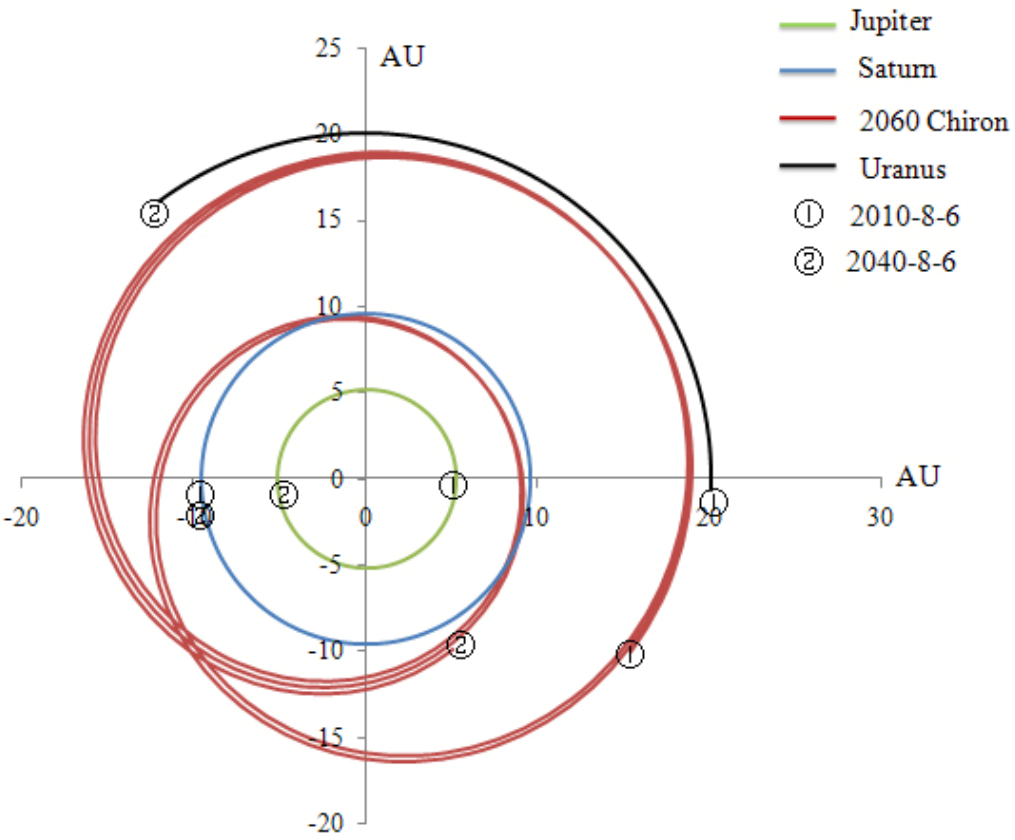

Figure 17: The orbit of 2060 Chiron at the plane of the elliptic. Time span is 30 years. The coordinate origin is solar system barycenter (ssb). ① represents the position of each body on 6 August 2010, while ② the position on 6 August 2040.

4 Discussion

Celestial objects are believed to be constrained by gravitational force to orbit, and the effect of gravitation is to drag object to mutually approach each other, thus with the passage of time the orbit of each celestial object will be forced to decrease, and then the collision between the two bodies of a two-body system is destined. But this kind of orbital decrease in the solar system is absolutely not easy to be found, the main reason is the Earth (observer) and other planets are located approximately at a plane, this makes radial distance measurement extremely difficult. Comparatively speaking, the orbital planes of stars and extrosolar planets are easy to be measured if they are approximately vertical to the line of sight. Another reason is that the amplitude of

orbital decrease during a limited time is too small to be detected. For instance, the Earth during a time of 100 years has an orbital decrease of less than 4 km (according to the experienced formula), the orbital decrease for other planets like the Mars, Jupiter, Saturn, and so during this period are even small. However, during a period of astronomical time this kind of orbital decrease is significant. Anyway, the observation of binary star systems, extrosolar planets, and the Phobos of Mars undoubtedly may confirm this existence of orbital decrease. In this paper, I use a geological record of coral fossil to deduce the amplitude of orbital decrease, many people must strongly dispute that the variation of the number of days recorded in the coral fossil is the consequence of a slowing Earth's rotation. About this question, I make an oral argumentation, accurate analysis is left to be done in the future. For the Earth-Moon system, the two bodies are orbiting around a common center of their mass. This rotation undoubtedly may result in a centrifugal effect for them, but because of the pull of gravitation, the Earth's body must be distorted into a prolate spheroid with major axis directed toward the Moon. The Earth is covered with water (around 71% the total area of the Earth's surface), the heavier component may be treated as be immersed in the bottom of the water. The Earth's volume is always conservative, this means that the heavier component due to a centrifugal effect will move away from the bottom of the water (away from the side of the Moon), this will automatically extrude the water to flow toward the side of the Moon. The sea level that faces the Moon is thus boosted. Due to the Earth's rotation, the tide per day must undergo a rise and fall. On the other hand, because the Earth-Moon system is orbiting around the Sun (actually around the barycenter of the third two-body system, see the work by Yang (2011)) and the barycenter of the Earth-Moon is geometrically located in the body of the Earth, the interaction of centrifugal effect and gravitation will again distorted the Earth's body in the direction of 3-O_1, the orbit of the Moon relative to the ecliptic has a little inclination, this means that two kind of gravitations and centrifugal effects during a Moon's round (around 30 days) may together distort the Earth's body greatly, once the Sun (the barycenter of third two-body system) and the Moon are at the same side of the Earth, sea level must be highly boosted, if they are at the opposite of the Earth, sea level must be highly counteracted, the tide per month thus undergoes an extreme height and low. However, the final result is determined by the interaction of a series of factors like sea water distribution, gravitation, and so on.

Among of the four giant planetary ring systems, the Jupiter's and Saturn's rings are very wide

and thin, this corresponds to a long time of radial spread. Contrary to this, the Uranus's rings are very narrow, which does a young age and a short time of evolution. In the solar system, the Earth has a satellite -the Moon. As of October 2009, more than 180 minor planets have been found to have moon (s) (reference to Johnston's Archive: Asteroids with Satellites). Each of four giant planets (Jupiter, Saturn, Uranus, and Neptune) generally holds a number of satellites, which makes it look like a small solar system. It is possible that some of these satellites in the past hold their own moons, but due to orbital shrinkage these moons had lost to the collision with their father satellites. Countless craters on the surfaces of planets and satellites suggest that they were severely bombarded after their formations but not before, this naturally requires some special events to responsible for. In recent years a number of irregular moons have been found to orbit the Jovian planets, they form some groups and families that are similar to the asteroids in the main belt (Huebner 2000). It is undoubtedly certain that these irregular moons are the fragments that were ejected from the collisional events. As a result, it is not difficult to distinguish conventional moons of giant planets from their irregular satellites according to physical feature. Conventional moons are generally round (spherical) and massive, and their orbits are standard-circular, and approximately parallel to planetary equatorial plane. For instance, Mimas, Enceladus, Tethys, Dione, Rhea, Titan, and Iapetus may be classified as the conventional moons of the Saturn, while the remaining should be the fragments of a previous binary satellite system; Io, Europa, Ganymede, and Callisto may be classified as conventional moons of the Jupiter, while the remaining should be the fragments of a previous binary satellite system； Miranda, Ariel, Umbriel, Titania, and Oberon may be classified as conventional moons of the Uranus, while the remaining should be the fragments of a previous binary satellite system; Triton may be classified as conventional moons of the Neptune, while the remaining should be the fragments of a previous binary satellite system. It is necessary to note that, because all fragments (irregular moons) are running parabolic trajectories around the barycenters in the rings, this determines that the orbits of irregular moons with respect to planet are highly eccentric and with respect to planetary equatorial plane are various inclinations. However, due to the successive drag of a series of hierarchical two-body systems, the inner irregular moons (close to planet) are easier to form low-inclination orbits than these outer irregular moons. The low density of Saturn's small moons and their spectral characteristics similar to those of the main rings, closeness to the rings and rapid disruptive

timescales have long suggested that their origin may be linked to the planet's icy rings (Jewitt et al. 2006; Nesvorny et al. 2003; Porco et al. 2007). It is generally believed that planetary rings are derived from the collisional fragmentations of a number of small bodies that once existed around the planet (Esposito 2002; Burns et al. 2001). The members of asteroid family (or group) are also thought to be the fragments produced by the disruption of a common parent body resulting from a catastrophic collision (Zappala et al. 2002). These instinctive understandings are often right and should be considered.

In the smashing collision, the ejected fragments due to the conservation of momentum will be symmetrically distributed around the barycenter of binary planetary system. This means that the average orbital radius of the fragments around the Sun is approximately equal to the planetary system's orbital radius around the Sun. We through JPL Small-Body Database Search Engine search for asteroids located at a range between Mars' and Jupiter's orbit (1.52AU <R<5.2 AU). Around 536818 asteroids are found and their average semi-major axis around the Sun and inclination with respect to the elliptic are worked out to be 2.67 AU and 8.30 degrees, respectively. At a distance of 2.67 AU from the Sun, the Sun's mass may determine an orbital period of 4.36 years. These should be the constraints of the barycenter (point *O*) of the previous binary planetary system orbiting the Sun at present. Titius-Bode Law has an experience expression of $a = (n+4)/10$ (where a is the semi-major axis of a planet around the Sun and n=0, 3, 6, 12, 24, 48 ...). Consider the distribution of established planets (like Mercury, Venus, Earth, Mars, Jupiter …) with respect to the Sun, the position of the proposed planetary system from this formula is expected to be $a = (24+4)/10 = 2.8$ AU. Our result is nearly equal to this expectation.

If such a smashing collision had occurred for the proposed binary planetary system in the past, a natural aftermath is that a large number of fragments would be ejected from the collisional source towards all around (reference to Figure 1(B)), and therefore can bombard the objects they encounter in the travel, and thereby leave craters and scrapes on the surfaces of these objects. In general, the nearer the objects are from the collisional source, the more the objects can encounter bombardment from the fragments. As shown in Figure 18, when the fragments from the collisional origin are ejected, the Mars and Earth in their orbits can inevitably be bombarded by some of the ejecting fragments. As the Mars is close to the collisional source more than the Earth, the Mars and its satellites can naturally receive more bombardment than the Earth and Moon can do. In

particular, the synchronous rotation of the Moon around the Earth can get its far side receive more bombardment than the near side. As stated previously in this paper, the ejected fragments under the effect of hierarchical two-body confinement can be dragged to fall on a circular belt, also because the Moon is a sphere and its orbit has an inclination of 5.15 degrees to the elliptic, this determines that the Moon in motion can repeatedly run through part of the fragment belt. In the course of penetration, the south and north poles of the Moon can inevitably collide with the fragments to leave heavy craters (Fig.19). We must remember that, because of the existence of orbital decrease, the Mars and Earth in the past should be more near to the asteroid belt than in the present. This means that both of them might have encountered more bombardment in the past than in the present. From Figure 18, we conclude, the satellites of the Mars (Deimos and Phobos) might had hold perfect spherical shape like the Earth's satellite- the Moon, but subsequently they were severely bombarded by the fragments and thereby left disabled structures, a heavy bombardment may also destroy the Mars's shroud if it is surrounded by thick atmosphere like what on the Earth, by which the climate system is seriously disturbed, for instance, water composition may escape toward outer space, and then wet climatic surroundings on the Mars disappears.

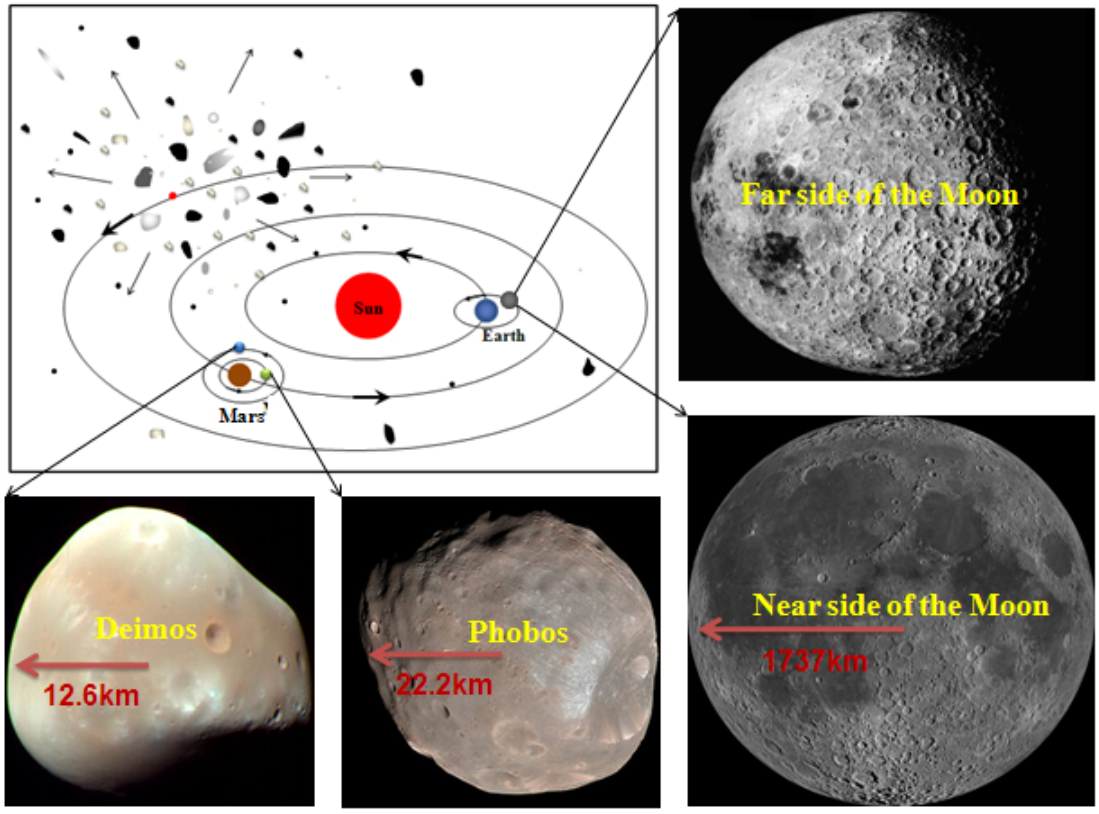

Figure 18: Ejecting fragments inward bombard planets and their satellites to form various

craters. Red dot in the model diagram represents the barycenter of the proposed planetary system. Images of Deimos, Phobos, far side of the Moon, and near side of the Moon are by the courtesy of NASA.

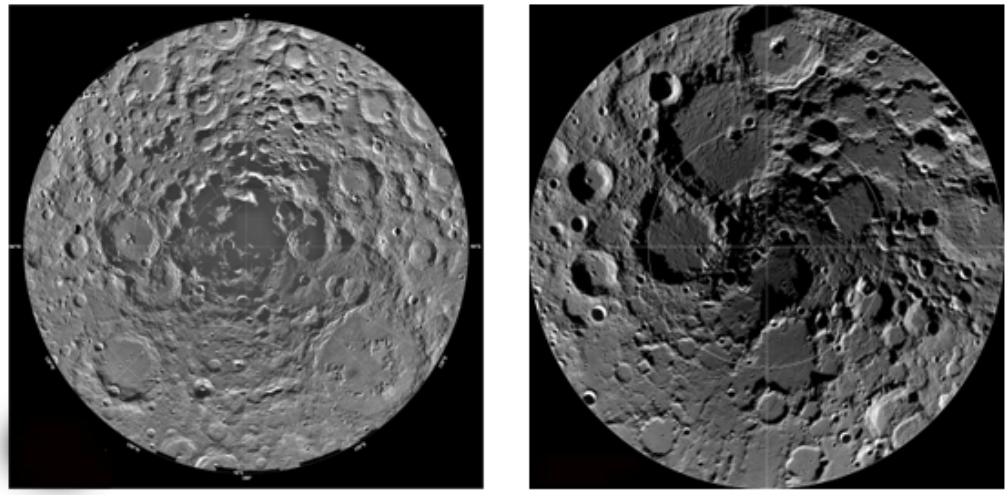

Figure 19: South (left) and North (right) Poles of the Moon. Images are by the courtesy of NASA/JPL/USGS.

A latest analysis of dust particles from near-Earth asteroid 25143 Itokawa shows that the asteroid is likely to be made of reassembled pieces of the interior portions of a once larger asteroid (Nakamura et al. 2011). This means that larger asteroids might have been further shattered into smaller asteroids. The impact crater record of the terrestrial planets and the Moon confirms an inner solar system impact cataclysm occurred 3.9 Gy ago, and identifies the main asteroid belt as the source of the impactors (Strom et al. 2005). The heavily crater surfaces on Ganymede and Gallisto discovered by Voyager 1 confirms another kind of bombardments occurred in the outer solar system (Strom et al. 1981). Possible causes proposed for these bombardments include gas giant migration (Gomes et al. 2005) and Late Uranus/Neptune formation (Levison et al. 2001). However, the story of gas giant migration has two uncertainties, the first is it assumed a rich trans-Neptunian belt to firstly interact with giant planets, but so far no evidence can support the existence of this trans-Neptunian belt, the second is it cannot account for the difference of crater distribution, for instance, on the Moon's surface there are more craters on the far side than on the near side, most importantly, the craters on the south and north poles appear to be more serious than on the near and far sides. The proposal of late Uranus/Neptune formation has not yet obtained

support from numerical simulation. In recent years NASA John Chambers and Jack Lissauer proposed a fifth planet (V) that exists between Mars and the asteroid belt to increase crater rate, but Planet V and its disruption are unclear, too. The comparison of cratering record from Mercury to Uranus shows that the solar system cratering record cannot be explained by a single family of objects in heliocentric orbits, e.g., comets (Strom 1987). All these problems strongly require a more compelling model to account for. In a private communication with professor Robert G. Strom, he stated that the younger population of crater has been accumulating from the end of the period of Late Heavy Bombardment about 3.8 -3.7 ba up to the present time. In this present paper we totally propose 5 collisional scenarios: one occurred in the inner solar system around 3.9 ba that yielded a large number of fragments to create the old population of craters (the Late Heavy Bombardment), other four independently occurred in the outer solar system after the Late Heavy Bombardment (later than 3.8 ba) that yielded a lot of fragments to create the younger population of craters, but as all fragments are running parabolic trajectories around the barycenters in the asteroid belt and planetary rings, they will gradually return to the asteroid belt and planetary rings, in this falling process an accumulating population of craters may be formed on the surfaces of planets and satellites. The collision of comet Shoemaker-Levy and Jupiter may be such a case.

A large number of meteorites in the past have been found on the Earth. The majority of the meteorites are chondrites, they are composed mostly of silicate minerals that appear to have been melted while they were free-floating objects in space. Even some types of chondrites contain small amounts of organic matter (Ceplecha et al. 1961). But the scenario that accounts for the origin of meteorite remains uncertain. The majority of meteorites are believed to come from the asteroid belt, some are thought to come from the Moon and the Mars due to the dispersion of impactors. Indeed, the chemical composition of the majority of meteorites is similar to that of the asteroids in the belt (plentiful carbonaceous and silicate material but less metallic material, for instance), but this needs a mechanism to explain how meteorites transport from the asteroid belt to the Earth. Carrying meteorites from the Moon and Mars to the Earth appears to be extremely difficult, because it needs to consider the connection of a series of transporting events. Moreover, meteorites have been found in different places, NASA's Opportunity Rover in 2005 captured an iron meteorite on the Mars. The collision of the two bodies of a previous binary planetary system may create such a condition for fragments to travel and land on the surfaces of planets and

satellites and further become meteorites. In the collision some melting materials (including rock and iron) in the bodies of the binary planetary system may be released and recrystallized, while some organic matter may be sealed in the voids of fragments.

According to Figure 3, the final velocity of a fragment is between $V_1+V_2 \sim V_1-V_2$, regardless of the influence of gravitation, this means the comet's velocity is various, namely some of the comets may hold very rapid speed in space. A rapid comet naturally requires a strong force to control, reference to Figure 14 and the work (Yang 2011), the Sun and all planets together are indirectly responsible for the motion of a comet through the barycenters of a series of hierarchical two-body systems, the requirement of a strong force for the comet may thus be satisfied. Most of comets are composed of water ice, rock, dust, and frozen gases (Poulet et al. 2003), planetary ring also consists of mainly water ice and dust. As of 2008, three centaurs such as 2060 Chiron, 60558 Echeclus, and 166P/NEAT have been found to display cometary coma (Coradini et al. 2009). This similarity indicates that both planetary ring and comet (centaur) could be related.

The gravitation between objects still follows an inverse-square law, but its expression is not direct but indirect. On the whole, a hierarchical two-body system may also be simplified into a two-body system. The object's mass and gravitational constant I use in this paper are from the estimation of Newton's gravity, but these approximate values may be utilized if relative calculation is operated. The collisional scenario of binary planetary (satellite) systems proposed in this paper provides a starting point to integrally consider the origin of asteroid belt, planetary ring, and comets, along with the formation of craters and meteorites, future work in both observation and numerical simulation may strengthen the expectation of this model. Several expectations are as follows: 1) the rings of each giant planet are with various inclinations, the narrow rings are slowly widening, and new rings are being created, especially for the Uranus's ring system; 2) the particles of each ring are as a body in motion, even though they are discontinuous in space. To some extent, the ring system of each giant planet is as a body in motion; 3) spacecraft will not encounter any direct attraction from celestial objects, except for the Earth.

Acknowledgments I thank my family for their great understanding and support in doing this work.

References

E. A. Roche, Acad. Sci. Lett. Montpelier. Mem. Section Sci. **1**, 243 (1847)

J. B. Pollack , A. S. Grossman, R. Moore, H. C. Jr. Graboske, Icarus **29**, 35 (1976)

S. Charnoz, A. Morbidelli, L. Dones, J. Salmon, Icarus **199**, 413 (2009)

L.Dones, Icarus **92**, 194 (1991)

R. M. Canup, Nature **000**,1 (2010)

W. Herschel, Philosophical Transactions of the Royal Society of London **97**, 271(1807)

J.-M. Petit, A. Morbidelli, J. Chambers, Icarus **153**, 338 (2001)

J. H. Oort, Bull. Astron. Inst. Neth.**11**, 91 (1950)

G. P.Kuiper, In Astrophysics: A Tropical Symposium, edited by J. A. Hynek. Mcgraw-Hill, New York, 357 (1951)

S. Charnoz, J. Salmon and A. Crida, Nature **465**, 752 (2010)

J. A. Burns, D. P. Hamilton, M. R.Showalter, B A S Gustafson, S F Dermott and H Fechtig (Berlin: Springer) pp 641 (2001)

P.Goldreich, S.Tremaine, Nature **277**, 97 (1979)

C. C. Porco, P. Goldreich, AJ. **93**, 724 (1987)

B. A. Smith, *et al*., Science **233** (4759), 97 (1986)

E. D. Miner, R. R. Wessen, J. N. Jeffrey, Planetary Ring System. Springer Praxis Books (2007)

B. A. Smith, et al., Science **246** (4936), 1422(1989)

H. Salo and J. Hänninen, Science **282** (5391): 1102(1998)

C. Dumas, et al., Nature **400** (6746), 733(1999)

B. Sicardy, et al., Nature **400** (6746), 731(1999)

F. Namouni & C. Porco, Nature **417**, 45(2002)

B. Sicardy & S. Renner, Bull. Am. Astron. Soc.**35**, 929(2003)

S. Renner & B. Sicardy, Celestial Mechanics **88**, 397 (2004)

M. M. Woolfson, Q. J. R. Astr. Soc. **34**, 1(1993)

N.Taishi, N. Yushitsugu, ApJ. **421**, 640 (1994)

AN. Youdin, F. N. Shu, ApJ. **580**, 494 (2002)

H. H. Klahr, P. Bodenheimer, ApJ. **582**, 869 (2003)

S. Inaba, G.W. Wetherill, M. Ikoma, Icarus **166**, 46 (2003)

G. Wurchterl, Kluwer Academic Publishers (2004), pp 67–96

M. Duncan, T. Quinn, S.Tremaine, ApJ, Part 2 -Letters **328**, L69 (1988)

H.H. Hsieh, D.Jewitt, Science **312**, 61(2006)

L. W. Esposito, Reports On Progress In Physics **65**, 1741 (2002)

I. d. Pater, H. B. Hammel, S. G. Gibbard, M. R. Showalter, Science **312**, 92 (2006)

R. G. Strom, et, al., Science **309**, 1847 (2005)

R. G. Strom, et, al., Journal of Geophysical Research **86**, 8659 (1981)

R. L. Kelley, *et. al*., ApJ, **268**, 790(1983)

A. Levine, *et. al.*, ApJ, **410**, 328(1993)

J. M. Weisberg, J. H. Taylor, Binary Radio Pulsars ASP Conference Series, Vol. TBD, 2004 eds. F.A. Rasio & I.H. Stairs

C. Terquem and J. C. B. Papaloizou, ApJ, **654**, 1110(2007)

A. Brunini & R. G. Cionco, Icarus **177**, 264(2005)

S. N. Raymond, R. Barnes, & A. M. Mandell, MNRAS **384**, 663(2008)

D. Charbonneau, *et al*., Nature **462**, 891(2009)

S. Clark, "Flights to Phobos"in New Scientist magazine, 30th January 2010

K. Hirayama, AJ. **31**, 185 (1918)

C. D. Murray, *et al*., Nature **453**, 739 (2008)

H. Hammel, Springer Praxis Books (2006), pp251-265

Y. F.Yang, Proceedings of the 18th annual conference of the NPA, College Park, Maryland University, USA, Vol.**8**, 712 (2011). viXra:1010.0042

E. F., Tedesco, F. –X., Desert, AJ, **123** (4), 2070(2002).

S. G. Love, D. E. Brownlee, AJ.**104** (6), 2236 (1992)

Y. Funato, et al., Nature **427**, 518 (2004)

D. D. Durda, et al., Icarus **170**, 243 (2004)

S. J. Weidenschilling, Icarus **160**, 212 (2002)

P. Goldreich, Y. Lithwick, & R. Sari, Nature **420**, 643(2002)

S. A. Astakhov, E. A. Lee, & D. Farrelly, Mon.Not. R. Astron. Soc. **360**, 401(2005)

R. M. Canup, Science **307**, 546(2005)

J. L. Margot, et al., Science **296**, 1445(2002)

W. J. Merline, et al., Asteroids III 289 (Univ. Arizona Press, Tucson, 2002)

D. C. Stephens, & K. S. Noll, AJ. **131**,1142 (2006)

L. W. Esposito, *et al*., Icarus **194**, 278(2008)

C. D. Murray, M. K. Gordon, S. M. Giuliatti Winter, Icarus **129**, 304 (1997)

C. C. Porco, *et al*., Space Sci. Rev. **115**, 363 (2004)

C. C. Porco, *et al*., Science **307**, 1226(2005)

C. D. Murray, et al., Nature **437**, 1326 (2005)

M. Duncan, T. Quinn, T. Scott, ApJ. **328**, L69 (1988)

Z. Sekanina, AJ. **95**, 911(1988).

J. Horner, N.W. Evans, Mon. Not. R. Astron. Soc. **000**,1 (2008)

W. F. Huebner, Earth, Moon, and Planets. **89**,179 (2000)

D. C.Jewitt, A. Delsanti, Solar System Update : Topical and Timely Reviews in Solar System Sciences. Springer-Praxis Ed (2006)

D. Nesvorny, J. L. A. Alvarellos, L.Dones, H. Fevison, AJ. **126**, 298 (2003)

C. C. Porco, *et al*., Science **318**, 1602 (2007)

V. Zappalà, A. Cellino, A. Dell'Oro, P. Paolicchi, In Asteroids III (W. F. Bottke Jr. et al., eds.), this volume. Univ. of Arizona, Tucson (2002)

T. Nakamura, *et al*., Nature **333**, 1113 (2011)

R. Gomes, H. F. Levison, K. Tsiganis, A. Morbidelli, Nature **435**, 466 (2005)

H, F.Levison, *et, al*., Icarus **151**, 286 (2001)

R. G. Strom, Icarus **70**, 517 (1987)

Z. Ceplecha, Bull. Astron. Inst. Czechoslovakia **12**, 21(1961)

F. Poulet, *et al*., Astron. Astrophys. **412**, 305 (2003)

A. Coradini, *et al*., Earth Moon Planets **105**, 289 (2009)